



TALLINN UNIVERSITY OF TECHNOLOGY
SCHOOL OF ENGINEERING
Electrical Power Engineering and Mechatronics

BALANCING BIPEDAL ROBOT MOVEMENT

Kahejalgse roboti liikumise tasakaalustamine

MASTER THESIS

Student: Mostafa Mohamed Mostafa Abdelrahman

Student code: 195036-MAHM

Supervisor: Prof. Gennadi Arjassov

Tallinn 2021

AUTHOR'S DECLARATION

Hereby I declare, that I have written this thesis independently.

No academic degree has been applied for based on this material. All works, major viewpoints and data of the other authors used in this thesis have been referenced.

"....." 20.....

Author:

/signature /

Thesis is in accordance with terms and requirements

"....." 20....

Supervisor:

/signature/

Accepted for defence

".....".....20... .

Chairman of theses defence commission:

/name and signature/

Non-exclusive licence for reproduction and publication of a graduation thesis¹

I, Mostafa Mohamed Mostafa Abdelrahman

1. grant Tallinn University of Technology free licence (non-exclusive licence) for my thesis "Balancing Bipedal Robot Movement"

supervised by Prof. Gennadi Arjassov.

1.1 to be reproduced for the purposes of preservation and electronic publication of the graduation thesis, incl. to be entered in the digital collection of the library of Tallinn University of Technology until expiry of the term of copyright;

1.2 to be published via the web of Tallinn University of Technology, incl. to be entered in the digital collection of the library of Tallinn University of Technology until expiry of the term of copyright.

2. I am aware that the author also retains the rights specified in clause 1 of the non-exclusive licence.

3. I confirm that granting the non-exclusive licence does not infringe other persons' intellectual property rights, the rights arising from the Personal Data Protection Act or rights arising from other legislation.

_____ (date)

¹ The non-exclusive licence is not valid during the validity of access restriction indicated in the student's application for restriction on access to the graduation thesis that has been signed by the school's dean, except in case of the university's right to reproduce the thesis for preservation purposes only. If a graduation thesis is based on the joint creative activity of two or more persons and the co-author(s) has/have not granted, by the set deadline, the student defending his/her graduation thesis consent to reproduce and publish the graduation thesis in compliance with clauses 1.1 and 1.2 of the non-exclusive licence, the non-exclusive license shall not be valid for the period.

THESIS TASK

Student: Mostafa Mohamed Mostafa Abdelrahman, 195036 MAHM

Study programme, MAHM02/19, Mechatronics

main speciality:

Supervisor(s): Prof. Gennadi Arjassov

Consultants:

Thesis topic:

(in English) Balancing Bipedal Robot Movement

(in Estonian) Kahejalgse roboti liikumise tasakaalustamine

Thesis main objectives:

1. Derivation of the mathematical equations of motion of the robot
2. Dynamically and Statically balance the robot while walking
3. Control the Vibration applied on the Bipedal Robot

Thesis tasks and time schedule:

| No | Task description | Deadline |
|----|---|------------|
| 1. | Derivation of Equation of motion of the robot | 30.03.2021 |
| 2. | Designing the robot 3D skeleton and Modeling the control system of dynamic and static balance | 21.04.2021 |
| 3. | Modeling the vibration control controller | 29.04.2021 |
| 4. | Analysis and Results | 10.05.2021 |
| 5. | Reviewing and finalizing the thesis paper Elements | 18.05.2021 |

Language: English **Deadline for submission of thesis:** "18" May 2021

Student: Mostafa Mohamed Mostafa Abdelrahman ".....".....2021
/signature/

Supervisor: Prof. Gennadi Arjassov ".....".....2021
/signature/

Consultant: ".....".....2021
/signature/

Head of study programme: Prof. Mart Tamre ".....".....2021
/signature/

Terms of thesis closed defence and/or restricted access conditions to be formulated on the reverse side

CONTENTS

| | |
|---|----|
| TABLE OF FIGURES..... | 7 |
| PREFACE..... | 9 |
| List of Abbreviations and Symbols | 10 |
| 1. INTRODUCTION..... | 11 |
| 2. LITERATURE REVIEW | 13 |
| 2.1 Locomotion Essentials..... | 13 |
| 2.1.1 Zero Moment Point Concept..... | 13 |
| 2.1.2 Center of Mass..... | 15 |
| 2.1.3 Center of Pressure | 15 |
| 2.1.4 Support Polygon..... | 16 |
| 2.1.5 Static and Dynamic Balance | 16 |
| 2.2 Gait Analysis | 17 |
| 2.2.1 Stance and Swing Leg | 17 |
| 2.2.2 Single and Double Support Phase | 18 |
| 2.2.3 Single Direction Walking and Omnidirectional Walking..... | 19 |
| 2.3 Balance Models | 19 |
| 2.3.1 Linear Inverted Pendulum | 19 |
| 2.3.2 Double Inverted Pendulum | 20 |
| 2.3.3 Spherical Inverted Pendulum | 21 |
| 2.3.4 Cart-Table Model..... | 22 |
| 2.3.5 Predictive Foot Placement Model | 23 |
| 2.4 Objectives of Thesis..... | 23 |
| 3. BALANCE STRATEGY..... | 25 |
| 3.1 Pre-defined Walking Gait..... | 25 |
| 3.2 Ankle Strategy | 25 |
| 3.3 Hip Strategy | 26 |
| 3.4 Stepping Strategy | 27 |

| | | |
|-------|--|----|
| 3.5 | Inverted Pendulum on Cart..... | 28 |
| 3.6 | Proposed Vibration Control Controllers | 32 |
| 3.6.1 | Fuzzy Logic | 32 |
| 3.6.2 | Linear Quadratic Regulator..... | 33 |
| 3.6.3 | Fuzzy Linear Quadratic Regulator | 33 |
| 3.7 | ZMP for Dynamic Balance | 34 |
| 3.8 | CoM for Static Balance | 34 |
| 3.9 | Model Predictive Control..... | 35 |
| 4. | DESIGN AND MODELING | 36 |
| 4.1 | Software Used | 36 |
| 4.2 | Bipedal Robot Design..... | 36 |
| 4.2.1 | Initial Design | 36 |
| 4.2.2 | Final 3D Design..... | 37 |
| 4.2.3 | Design Details..... | 38 |
| 4.3 | Modeling | 40 |
| 4.3.1 | Dynamic and Static Model | 40 |
| 4.3.2 | Vibration Control Model | 42 |
| 5. | SIMULATION AND ANALYSIS RESULTS..... | 44 |
| 5.1 | Dynamic and Static Balance Simulation | 44 |
| 5.2 | Dynamic and Static Balance Results..... | 48 |
| 5.3 | Vibration Control Simulation | 53 |
| 5.4 | Vibration Control Analysis Results..... | 54 |
| 5.5 | Maximum Pelvis Mass Stability | 57 |
| 5.6 | Future Work | 58 |
| | SUMMARY | 60 |
| | KOKKUVÕTE..... | 61 |
| | LIST OF REFERENCES | 62 |

TABLE OF FIGURES

| | |
|---|----|
| FIGURE 2.1: VCP PLANE [4] | 14 |
| FIGURE 2.2: LOCATION OF ZMP AND COP IN THE FOOT [5]..... | 14 |
| FIGURE 2.3: THE POINT OF PRESSURE IN THE FOOT WHILE CONTACTING THE GROUND [5] | 15 |
| FIGURE 2.4: SUPPORT POLYGON AREA AROUND THE FEET [6] | 16 |
| FIGURE 2.5: CASSIE ROBOT DYNAMICALLY AND STATICALLY BALANCED ON ROUGH TERRAIN [4]... | 17 |
| FIGURE 2.6:GAIT DESCRIPTION IN ORTHOPEDICS SCIENCE [7] | 18 |
| FIGURE 2.7:ILLUSTRATION OF SSP AND DSP WALKING [8] | 18 |
| FIGURE 2.8: BHR-5 ROBOT PERFORMING OMNIDIRECTIONAL MOVEMENT [9] | 19 |
| FIGURE 2.9: LINEAR INVERTED PENDULUM [11] | 20 |
| FIGURE 2.10: 3D MODEL OF BATH BIPEDAL HOPPER [12] | 20 |
| FIGURE 2.11:DOUBLE PENDULUM [12] | 21 |
| FIGURE 2.12: 2 DOF INVERTED PENDULUM [13] | 22 |
| FIGURE 2.13: ROBOT NAO IS AN EXAMPLE OF CART-TABLE MODEL [14] | 22 |
| FIGURE 2.14: ROBOT DRC HUBO FOOT PLACEMENT TEST [16]..... | 23 |
| FIGURE 3.1: ANKLE STRATEGY [4]..... | 26 |
| FIGURE 3.2: HIP STRATEGY [4] | 27 |
| FIGURE 3.3: CAPTURE POINT [4] | 28 |
| FIGURE 3.4: INVERTED PENDULUM ON A CART [19] | 29 |
| FIGURE 3.5: FUZZY LOGIC MODEL CONCEPT [20] | 32 |
| FIGURE 3.6: ZMP FOR DYNAMIC STABILITY [14]..... | 34 |
| FIGURE 3.7: CENTER OF MASS DIAGRAM [14]..... | 35 |
| FIGURE 4.1: INITIAL SKELETON DESIGN OF THE RAPTOR DINOSAUR MADE WITH CARDBOARD 4MM .. | 37 |
| FIGURE 4.2:THE FINAL 3D DESIGN OF THE RAPTOR DINOSAUR..... | 37 |
| FIGURE 4.3:THE RAPTOR DINOSAUR MAIN DIMENSIONS | 38 |
| FIGURE 4.4:LEG DOFs DETAILS..... | 39 |
| FIGURE 4.5:PELVIS AND HIP CONNECTION | 39 |
| FIGURE 4.6:HIP AND CALF CONNECTION..... | 39 |
| FIGURE 4.7:CALF AND FOOT CONNECTION | 40 |
| FIGURE 4.8:DYNAMIC AND STATIC BALANCE MODEL | 40 |
| FIGURE 4.9:WALKING CONTROLLER SUBSYSTEM | 41 |
| FIGURE 4.10:VIBRATION CONTROL USING LQR MODEL | 42 |
| FIGURE 4.11:LQR CONTROLLER | 43 |
| FIGURE 4.12:PLANT BLOCK..... | 43 |
| FIGURE 5.1: MOVEMENT FRAMES | 45 |
| FIGURE 5.2: THE BALANCING FACTORS..... | 46 |
| FIGURE 5.3: STEPPING LOGIC BLOCK | 47 |

| | |
|---|----|
| FIGURE 5.4: THE MULTIBODY MODEL..... | 47 |
| FIGURE 5.5: ACTUAL xZMP VS. TIME..... | 48 |
| FIGURE 5.6: yZMP VS. TIME | 49 |
| FIGURE 5.7: xCOM VS. TIME..... | 49 |
| FIGURE 5.8: yCOM VS. TIME | 50 |
| FIGURE 5.9: ANKLE ROLL DYNAMIC TIMES RESPONSE | 51 |
| FIGURE 5.10: ANKLE PITCH DYNAMIC TIME RESPONSE..... | 51 |
| FIGURE 5.11: KNEE ROLL DYNAMIC TIMES RESPONSE..... | 52 |
| FIGURE 5.12: HIP ROLL DYNAMIC TIME RESPONSE..... | 52 |
| FIGURE 5.13: HIP PITCH DYNAMIC TIMES RESPONSE..... | 53 |
| FIGURE 5.14: CART LINEAR DISPLACEMENT VS. TIME | 55 |
| FIGURE 5.15: LINK ANGULAR DISPLACEMENT VS. TIME..... | 55 |
| FIGURE 5.16: CYCLIC EXTERNAL DISTURBANCE CONTROL GRAPH FOR Q1..... | 56 |
| FIGURE 5.17: CYCLIC DISTURBANCE FOR ANGULAR DISPLACEMENT OF THE LINK Q2 | 56 |
| FIGURE 5.18: ANKLE ROLL JOINT VS TIME | 57 |
| FIGURE 5.19: HIP ROLL JOINT VS TIME..... | 57 |

PREFACE

The thesis topic aims to find a scientific method of solving the problem of bipedal robots balance. It is very challenging to make the robot walking balanced dynamically and statically. Several aspects have been deeply studied in this thesis to come up with a proper and updated solution with minimal errors to balance the bi-legged robots and recover from external perturbations along with making the proper steps to keep the balance.

I would like to thank the dean of department of mechatronics engineering, Prof. Mart Tamre, for his continuous support and advice from the first day I had joined the program to make this thesis topic happen. Thank you Professor Mart for believing in this topic and in my capabilities and flourishing the options and tools to make this thesis happen.

I would like also to thank the thesis supervisor Professor Gennadi Arjassov for his powerful knowledge, support and input in the dynamics and physics without which I couldn't have gone through these scientific methods to come up with those results. Nevertheless, Professor Gennadi has always been there daily supporting and standing by me like a father encouraging me in order to keep going in this hard challenging topic which positively affected the quality of work throughout the entire thesis phases.

I would like to thank all professors in all the mechatronics master's program for making me reach this level of knowledge and empowering me with methods and science. Thank you dear professors for making me who I am today.

Special thanks to Eng. Even Sekhri for his professional feedback and advice to me in order to come up with such a good thesis professional writing.

Finally, I would like to dedicate this paper to my mother and my fiancée for their great love, support and patience with me during this hard period of thesis.

List of Abbreviations and Symbols

| | |
|------|-------------------------------------|
| ZMP | Zero moment Point |
| DOF | Degree of Freedom |
| CoM | Center of Mass |
| CoF | Center of Pressure |
| LIPM | Linear Inverted Pendulum Model |
| IPM | Inverted Pendulum Model |
| SIP | Spherical Inverted Pendulum |
| IMU | Inertial Measurement Unit |
| CP | Conical Pendulum |
| PID | Proportional Integrated Derivative |
| DIP | Double Inverted Pendulum |
| SSP | Single Support Phase |
| DSP | Double Support Phase |
| VCP | Virtual Contact Surface Plane |
| GCoM | Ground Projection of Center of Mass |
| EZMP | Extended Zero Moment Point |
| FZMP | Fictitious Zero Moment Point |

1. INTRODUCTION

Robots have always been the image of science and technology for most people. People always dream to find robots moving like humans and rather doing their tasks in real life. Hollywood movies with the inspirations and the imaginations of directors even show how the robots would move, act and behave like human beings in real life. Such a movie like I-Robot showed how the two-leg humanoid act and behave in a fast and efficient way in different tasks of the human being in the future.

According to the robotic productions and courses, robots have been categorized in three different categories such as the industrial arm robot, the wheeled robot and legged robot. The industrial robot is mainly the robotic arm that has a certain identified task to do as machinery in the industrial area, such as factories, in order to perform a certain identified task of production with high speed and accuracy. This kind of robots is saving labor cost and further is capable to perform risky and exhausting different tasks in the production cycle in a fast and accurate way. The wheeled robot are basically robotic vehicles that move with wheels on flat terrain guided by joysticks or autonomously in order to perform a certain task such as delivery or mining or even detecting something in dangerous areas where it is harmful for human beings to go there. The legged robots are robotic skeletons that moved using N-number of legs. There are octa-legged robots that have 8 legs like spiders. There are hexa-legged robots that have 6 legs like some kinds of insects. There are Quadro-legged robots that have 4 legs like most of the animals and mammals. And finally, there are bi-legged robots like human beings or some animals or even birds. The less legs the robot has, the more complicated to control the movement of the robot.

Two-Legged robots or biped robots have been recently the main concentration of the scientists and researches for the complications and dynamics problems of the movement and stability. Unlike the wheeled robots, biped robots can act like human beings in performing certain tasks such as going on stairs or walking on rough and uneven terrains. However, the evaluation of the biped movement efficiency is based on going from point A, which is the initial starting point, to point B, which is the goal final point, without falling and fully controlling its movement against any external disturbance or perturbation coming to any of its edges.

Recently, there are such promising bipedal robots that have inspired us. Honda ASIMO, CASSIE of Oregon university [1], NAO of Aldebaran [2] and DLR of the Institute Robotics and Mechatronics in Germany [3] and definitely the Boston Dynamics bipedal famous

ATLAS robot have inspired me personally with the agility, mobility and stability of the skeleton while walking or standing still regardless the tested disturbances.

Last year, the author has tried to develop in the mechatronics smart systems course, supervised by Prof. Mart Tamre, a raptor dinosaur robot with 2 legs to make it walk, act and behave like a real dinosaur. The robot skeleton was done by cardboard of thickness of 4 mm, has been controlled by 2 Arduino microcontrollers and essential sensors and motors to make a smooth simultaneous movement of the 2 legs. However, the robot couldn't succeed to walk more than 6 steps and then fell.

It was then a motivation to continue in this field to rather study and come up with the balancing method in order to maintain the bipedal movement of a robot stable and balanced while standing still or walking regardless the external disturbance and the type of terrain the robot may walk on. In this thesis, the author will study and examine the balancing concept and strategies to tackle this problem for the biped type robot.

2. LITERATURE REVIEW

2.1 Locomotion Essentials

In this chapter, the author will illustrate the different approaches and methods of the scientists and those who conducted research in the field of balancing the bipedal movement of robots. These recent research papers were either presented in recent conferences or journals or even as doctorate theses. Mostly, in these researches and experiments that have been conducted, balancing of the bipedal robots was based on the combination of ZMP and CoM together to control the dynamics of the gait.

2.1.1 Zero Moment Point Concept

The Zero Moment Point concept is explained (ZMP) as a point on ground where the total moment generated due to inertia and gravity are zero [4]. ZMP concept is known for dynamic stability measurement of bipedal robots [2]. It was introduced in 1968 by Miomir Vukobratovic [2]. It is important that there is enough friction on ground to avoid slipping the single support phase foot. ZMP can be expressed as follows [2]:

$$p_x = \frac{\sum_{i=1}^n m_i(\ddot{z}_i+g)x_i - \sum_{i=1}^n m_i\dot{x}_i z_i - \sum_{i=1}^n I_{iy} \ddot{\theta}_{iy}}{\sum_{i=1}^n (\ddot{z}_i+g) m_i} \quad (2.1)$$

$$p_y = \frac{\sum_{i=1}^n m_i(\ddot{z}_i+g)y_i - \sum_{i=1}^n m_i\dot{y}_i z_i - \sum_{i=1}^n I_{ix} \ddot{\theta}_{ix}}{\sum_{i=1}^n (\ddot{z}_i+g) m_i} \quad (2.2)$$

Equation 2.1 and 2.2 express x_i , y_i and z_i as the position of the Center of Mass (CoM) of link i in cartesian coordinate system where z- axis is pointing up. g is the acceleration of gravity and m_i is the mass of link i . I_{ix} and $\ddot{\theta}_{ix}$ are the centroid moment of inertia and angular displacement with respect to the x and y axes, respectively [2].

There is another type of ZMP which is EZMP, the extended zero moment point, which is expressed as a point on a virtual contact surface in an arbitrary virtual surface with a finite slope [4]. This extension is used when the ground on which the bipedal robot is walking is rough and complex.

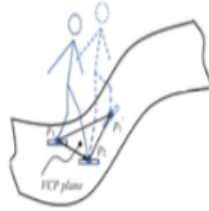


Figure 2.1: VCP Plane [4]

Figure 2.1 illustrates the rough terrain with an example of slope. For this kind of grounds EZMP model is rather used to keep the gait stability. If the ground is smooth then ZMP and EZMP are the same.

There is another type of ZMP which is FZMP (fictitious zero moment point) which is used for balancing when the ZMP is out of the convex hull of the support polygon. It is also used when the ground on which the robot walks is very smooth with very low friction. The following Figure 2.2 is the illustration of the ZMP and CoP (Center of Pressure) in the foot.

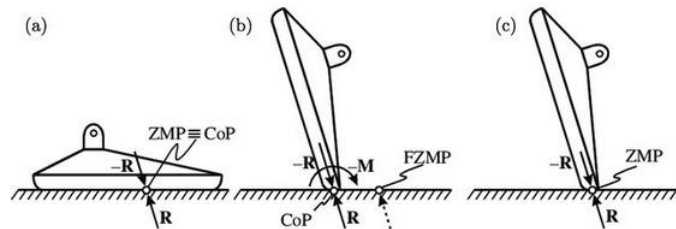


Figure 2.2: Location of ZMP and CoP in the foot [5]

Picture (a) in Figure 2.2 shows the state where the foot is fully on the floor. The convex hull of the support polygon is around the foot. The center of pressure is the same as zero moment point in the same point of contact between the foot and the ground because this is the state of stability of the foot meaning that it is dynamically balanced[5]. Picture (b) in Figure 2.2 shows when the foot is unstable and the bipedal robot is about to fall. In this case, the center of pressure is the point of the contact between the foot and the ground since that the center of pressure remains always the contact point. However, the ZMP went outside of the support polygon and has become Fictitious zero moment point. Thus, ZMP and CoP in picture (b) are not located in the same point since that it is unbalanced gait [5]. Finally, picture (c) in Figure 2.2 shows the tiptoe scenario where ZMP is the contact point. It is called Balletic motion [5].

2.1.2 Center of Mass

The center of mass for a distributed mass of an object is the unique point where the weighted relative mass of the distributed mass sums to zero [4]. It is also referred to as balance point since that theoretically speaking the entire mass of the object is concentrated in one point. Calculating each mass of each part in the robot is quite complex. Thus, to simplify mechanical calculations, it is easier to set the center of mass as a reference point.

2.1.3 Center of Pressure

The center of pressure for bipedal robots is the point on the surface of the ground where the ground reaction force act [2]. It can be also defined as the point where the resultant moment generated by the inertial gravity and the gravity forces is tangential to the surface where the final result in the horizontal plane is zero [2].

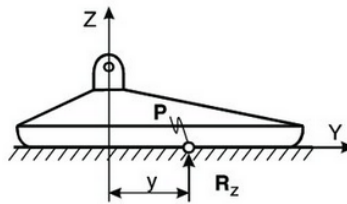


Figure 2.3: The point of pressure in the foot while contacting the ground [5]

Figure 2.3 shows the location of the center of pressure when the foot is fully on ground. As previously explained, the center of pressure is the contact point between the robot foot and the surface. When the robot is expressed as dynamically balanced gait, the center of pressure is almost located around the center of convex hull of the support polygon as shown in Figure 2.3 [5].

When the robot is in a balanced state both ZMP and CoP are in the same point in the polygon area. In any state of stability, the CoP doesn't leave the polygon area. Center of pressure can be expressed as follows [4]:

$$OP = \frac{\sum_{i=1}^N q_i F_{ni}}{\sum_{i=1}^N F_{ni}} \quad (2.3)$$

Equation 2.3 expresses OP as the vector from the origin of the coordinate system O to the center of pressure position and q_i as the vector to the point where F_{ni} acts in the perpendicular to the surface (Z direction) [2].

2.1.4 Support Polygon

One of the stability factors for a biped robot is the support polygon [6]. The support polygon is the horizontal area on the ground where during single support phase or double support phase the footprint is existing. It is described as the convex hull of the robot footprint. This area defines the static stability of the robot if the center of mass is existing inside of the support polygon area. When there is a double support phase, the robot has a more static stability. The larger the foot dimension is the more stable the robot is.

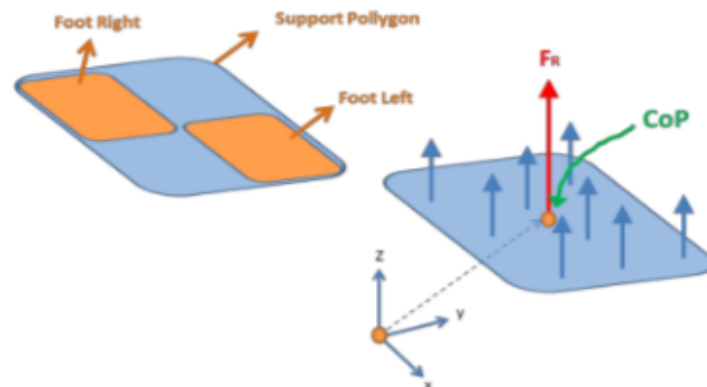


Figure 2.4: Support polygon area around the feet [6]

Figure 2.4 illustrates graphically the area around the right and left feet in which the CoP is located. The support polygon is the area in which ZMP and CoM should exist during the walking gait in order to maintain the dynamic and static balance of the robot.

2.1.5 Static and Dynamic Balance

Static balance of a biped robot is when the ground projection center of mass is remaining in the support polygon area. This means that the gravity line of the center of mass is in the center of the support polygon area. If the robot is standing and the ground projection of center of mass leaves the polygon area, this may cause the robot to fall. Static

balance is therefore measured proportionally according to the distance between the GCoM and the polygon area edge. On the other hand, the dynamic balance is when the ZMP is in the polygon area and putting into consideration the measurement between the polygon edge and the ZMP while walking. This kind of movement balance is similar to human beings dynamically [2].



Figure 2.5: Cassie Robot Dynamically and Statically Balanced on Rough Terrain [4]

Figure 2.5 shows how Cassie robot could balance itself dynamically and statically on a rough terrain by keeping ZMP and CoM in the support polygon.

2.2 Gait Analysis

2.2.1 Stance and Swing Leg

Stance phase is defined as when the leg gets in contact with the surface of the ground and leaves it; while swing phase is defined as when the leg leaves the surface of the ground until it gets in contact with the surface again [7]. As described in Figure 2.6, the stance phase is almost 60 percent of the walking while the swing is the remaining 40 percent of the walking.

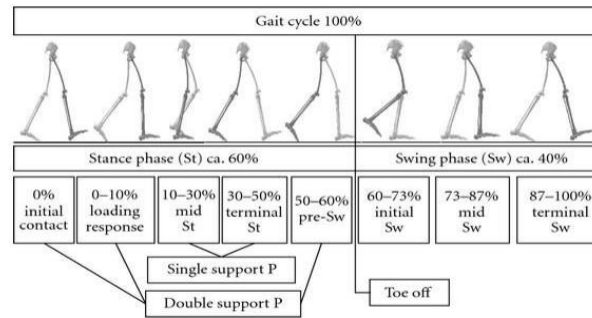


Figure 2.6:Gait Description in Orthopedics Science [7]

2.2.2 Single and Double Support Phase

Single support phase is explained as one of the bipedal robot legs that is in contact with the ground and supporting the robot's weight; while the double support phase [8] is when both legs are in contact with the floor creating a more stable state through an enlarged area of support polygon [4]. Following is the illustration of the SSP (Single Support Phase) and DSP (Double Support Phase).

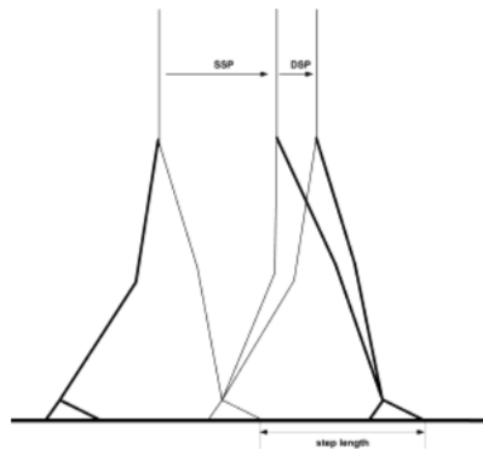


Figure 2.7:Illustration of SSP and DSP walking [8]

As it is shown in Figure 2.7, double support phase happens in the time interval where both feet are in contact with the ground; while the single support phase as shown is when one leg is on the floor supporting the weight and the other leg is moving [8].

2.2.3 Single Direction Walking and Omnidirectional Walking

A single direction walking gait is when the robot moves in a straight line. Omnidirectional walking makes the bipedal robot move in diagonal, curved or even sideways [4]. The single direction walking is not practical since that the robot cannot perform all the scenarios of the real human beings with their instant reactions and finding better path to avoid obstacles. However, the omnidirectional walking allows the robot to move smoothly like human beings in complex dynamic environments. It is important while developing the omnidirectional walking robot to connect the CoM with the new direction of movement and also to keep stability control since that the ZMP gets to the margins of the support Polygon [4].

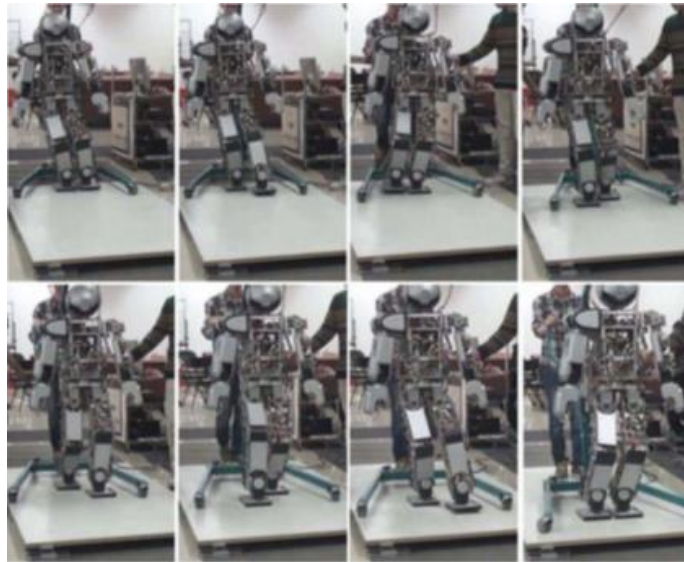


Figure 2.8: BHR-5 Robot performing omnidirectional movement [9]

Figure 2.8 shows the experiment in [9]. The robot BHR-5 has been tested for balance before performing the omnidirectional movement in different inclined environments.

2.3 Balance Models

2.3.1 Linear Inverted Pendulum

The linear inverted pendulum is a physical model that is being used for biped robot balance. Through its simplified equations, it assumes that there is one mass point in the

CoM [10]. It also assumes that the pendulum motion is in the horizontal plane without any vertical movement. According to the LIPM, the ZMP is set to the ankle point where the torque is zero. The drawback is that it neglects the angular momentum.

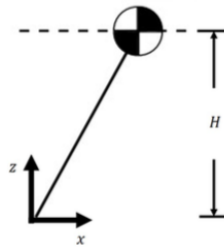


Figure 2.9: Linear Inverted Pendulum [11]

Figure 2.9 illustrates the linear inverted pendulum model which consists of pendulum mass and the rod.

2.3.2 Double Inverted Pendulum

The double inverted pendulum is the combination of inverted pendulum and the double pendulum [12]. The double inverted pendulum can fall unless it is controlled by moving; while the base as for inverted pendulum and torque is being applied at the pivot point between both pendulums. Ding et al. [12] has experimented in his research the use of double inverted pendulum on Bath Bipedal Hopper which is actuated by hydraulic. The physical system has one upper body and a two-leg coupled together like Kangaroo. The hydraulic cylinder actuates the fore-aft hip rotation of both legs [12]. The drawbacks were the measurement noises affecting the control signal.

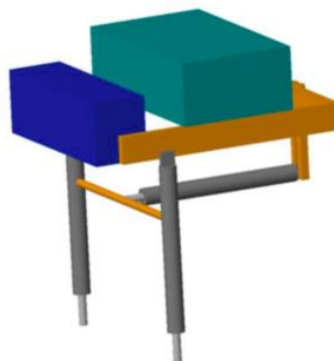


Figure 2.10: 3D model of Bath Bipedal Hopper [12]

Figure 2.10 shows the 3D design of the bath bipedal hopper with the hydraulic cylinder that was experimented in the research [12]. Figure 2.11 illustrates the concept of double pendulum [12].

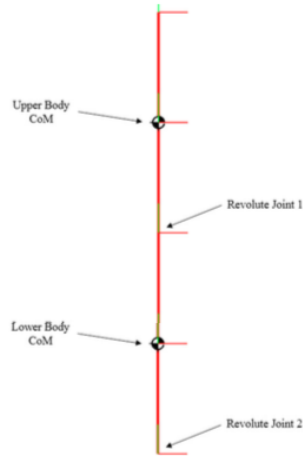


Figure 2.11: Double Pendulum [12]

2.3.3 Spherical Inverted Pendulum

The spherical inverted pendulum is a type of pendulum that is assuming the total mass of the robot is at the CoM. The point mass is supported with a link that is the stance leg of the robot that doesn't have mass; and the sole contact point with the ground is the ankle joint [13]. The ankle joint is assumed to be a 2 DoF rotational joint to let the CoM point move in a 3D space. The CoM moves freely within the space with no requirements to CoM height and no friction in sphere. The only force on the mass is the reaction of the sphere and the gravity. This makes it more of smooth motion. Elhaisri et al. [13] has experimented this new concept and concluded that the drawback is with the tuning of the control gain.

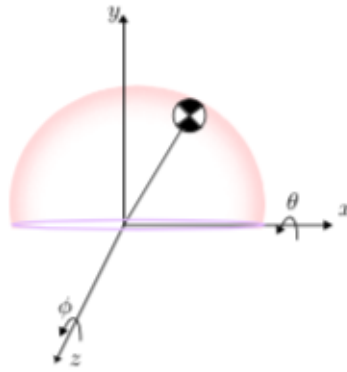


Figure 2.12: 2 DoF Inverted Pendulum [13]

Figure 2.12 is illustrating the spherical inverted pendulum in a 3-dimension space.

2.3.4 Cart-Table Model

The cart-Table model is a model that is used for simplifications. It assumes that all the masses of the robot are concentrated on the cart [2]. It also assumes that the leg doesn't have any mass. Even though it is not real, yet while developing a bipedal robot, usually the components are being put in the pelvis so that the other masses are relatively small compared to the center of the robot. The drawback is that it doesn't put into consideration the angular momentum which is essential for dynamic balance.



Figure 2.13: Robot NAO is an example of cart-table model [14]

Figure 2.13 shows an example of cart-table model application which is the robot NAO. This robot has proven its success of balancing the bipedal robot dynamically and statically.

2.3.5 Predictive Foot Placement Model

The Predictive foot placement model is based on linear inverted pendulum on swing leg dynamics. It aims to predict the next foot step to recover balance against the external perturbation. Zhang et al. [15] experimented the predictive foot placement model by expanding the LIPM with actuated LP mounted in pelvis. With considerations of swing capability, including the finite swing torque and zero-velocity landing of swing foot, it could provide more reliable predictions of foot placement in practical environments. Optimal step duration keeps constant under various perturbation; and, step position increases linearly with the magnitude of perturbations [15]. This model is a recent one and still under test.

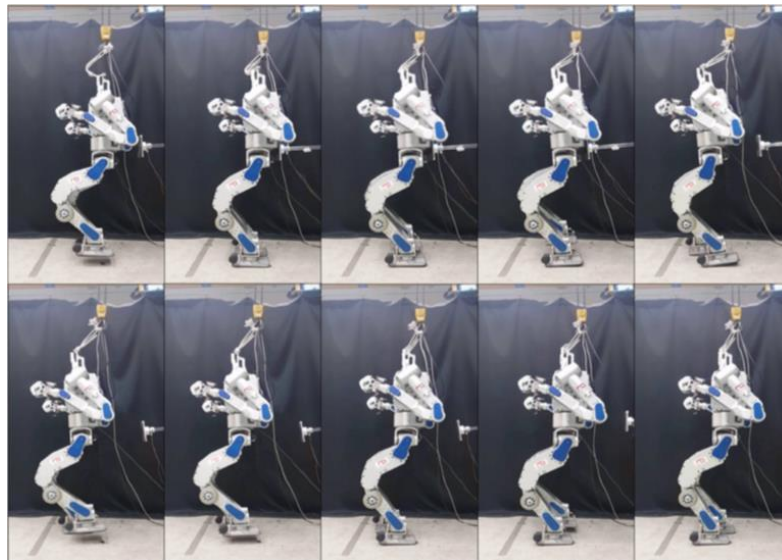


Figure 2.14: Robot DRC HUBO foot placement test [16]

Figure 2.14 shows the test of the robot DRC HUBO in [16] as predicting the next foot step and how it performs the foot placement concept to avoid falling.

2.4 Objectives of Thesis

According to the papers review, to have a static and dynamic balance, such models as ZMP and CoM should be taken into consideration in the balance control. Keeping the GCoM in the support polygon convex hull gives it the static balance; while, keeping the ZMP for dynamic balance will make the bipedal robot having stability in the walking gait. There are lots of papers and research in which scientists have conducted several

experiments with additional models in the last decades in order to maintain the balance of robots against the external perturbations and with respect to the different terrain types whether smooth or rough or complex or even slippery. Such models have been proposed like LIP and DIP and SIP in order to control the balance problem in the environment of perturbations. However, there is always a drawback in which there is a noise or vibration or a slow foot placement from which the robot falls while testing.

It is important to develop a pre-defined walkin gait about how the robot should walk first since that we are looking to have the bipedal robot acting and behaving as human beings with no limits. Thus, it is crucial to put first the balance strategies from which the robot's balance is being set.

In the third chapter, the author shall illustrate the balance strategies that have been put to the bipedal robot. In the fourth chapter, the author shall explain in details the design of the robot and the models that have been created in order to control the balance. In the fifth chapter, the simulation analysis and results and the future works shall be further explained into details. Finally, the paper will end up with the summary in which the whole thesis work will be concluded.

3. BALANCE STRATEGY

3.1 Pre-defined Walking Gait

The author has assumed that the bipedal robot will walk in a straight-line direction. It is also assumed that the total mass is in the pelvis and that the legs are massless. The bipedal robot was designed has 12 degrees of freedom in both legs; where, there are 6 degrees of freedom in each leg (hip 3, knee 1, ankle 2). Dimensions of each leg link, pelvis and foot are further explained in the design section in the next chapter. The author assumed that the external perturbations will be applied in a lateral direction on pelvis while being in the SSP. There are SSP, DSP1 and DSP2 in the gait trajectory. The overall SSP walking time is 14.2 seconds.

3.2 Ankle Strategy

It is very challenging to keep the bipedal robot balanced while walking. There are several disturbances that may occur on the robot whether sudden external perturbations applied on the pelvis of the robot that may push it to fall or continuous perturbations while walking on a rough terrain. It is therefore crucial to set a push off recovery or balance strategy in order to keep the robot from falling on ground. Ankle strategy aims to stabilize the robot against the slight disturbances applied on the robot. Such strategy is made by adding torque to the ankle joints to tackle the small disturbance applied on the robot while being in the SSP or DSP phases. Ankle strategy is basically responsible for the static balance of the robot. In order to keep the static balance, the system has to keep the GCOM (ground projection of the center of mass) in the support polygon (SP).

Bahdi et al. [4] has stated in his paper that applying ankle strategy is by increasing the ankle stiffness so that the robot keeps the center of pressure in the middle of the support polygon. He also concluded that using force sensors in the feet can estimate that needed torque for the ankle joint in order to keep the CoP in the SP. Bahdi et al. [4] has proved that the ankle strategy, as a recovery strategy, succeeded in balancing statically the inverted pendulum. Reimann et al. [17] proposed in his biomechanical model that the ankle strategy should be lateral strategy in order to act like human beings while

preventing the fall on ground since that human beings tend to use the lateral ankle when they are about to fall down in real life. Reimann et al. [17] also added that this suggested strategy allows the robot to control the CoM all the time and not only during the walking. Lateral ankle strategy reduces the ground pressure under the foot since that it shifts the CoP away from the pull by changing the roll angle of the body segment to the direction of the pull. Reimann et al. [17] concluded that lateral ankle strategy helps with the foot placement strategy in the stepping strategy.

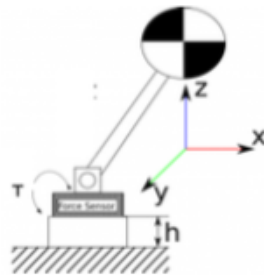


Figure 3.1: Ankle Strategy [4]

Figure 3.1 illustrates the ankle joint and how the torque will be further added and applied in order to keep the GCoM in the support polygon to balance the robot statically. Ankle Strategy nevertheless will help to keep the CoP in the support polygon since that it affects the ground projection of center of mass.

Ankle strategy is limited to small disturbances and thus it needs the hip joint to help when the disturbance can't be controlled.

3.3 Hip Strategy

Hip strategy is known in the robotics as the momentum strategy. When the ankle strategy fails to handle the extra disturbance, the hip helps with the hip joints since that they have higher torque to move the upper body part so that the CoP remains in the support polygon. Reimann et al. [17] in his biomechanical model stated that the hip strategy helps to pull the trunk through its higher torque in the hip joints which enables the adjustment of the CoM since that it exists in the trunk. He added that the ankle acceleration is clockwise while the hip acceleration is counterclockwise which is an additional mechanism to keep the CoM in the support polygon and keep the robot balanced statically. Bahdi et al. [4] stated that the hip strategy is useful for higher

perturbation since that it aims to move the CoM towards the CoP to make them almost aligned in the same point in the center of the support polygon.

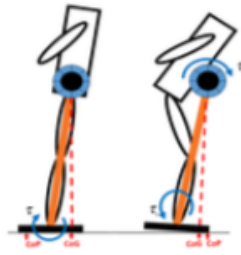


Figure 3.2: Hip Strategy [4]

Figure 3.2 illustrates how the hip joints pull the trunk to make the center of mass closer to the center of pressure.

3.4 Stepping Strategy

Stepping strategy is responsible to balance the bipedal robot when the external forces are applied on the robot and that the robot is about to fall. Reimann et al. [17] in his biomechanical model applied the foot placement model as a part of the stepping strategy. He concluded that if during the stance phase the robot is pushed towards the stance leg direction, the robot makes a step towards the same direction of the push because the CoM goes to that direction; and thus, the robot will keep the CoM in the support polygon.

Bahdi et al. [4] in his paper illustrated the importance of the stepping strategy. He explained that if the force applied on the robot is applied, it may push quickly the CoM to outside of the support polygon which makes it unstable. He stated that the robot in that state may need one or two steps forward in order to balance itself back again or alternatively go to DSP to maintain balance. Bahdi et al. [4] added that the modern stepping strategy is to apply capture point concept which helps the robot to make the correct step in which the CoM will be in the support polygon and the robot gets balanced back again. Zhang et al. [15] explained the importance of capture point as a point on the ground where stability is achieved. It is a recovery step to make the robot stand and get back the steady-state using swing leg. Shafiee-Ashtiani et al. [18] developed in his model MPC in order to keep the capture point along with the CoM and CoP within the

support polygon so that the robot knows the best step to take when a push is applied on the trunk.

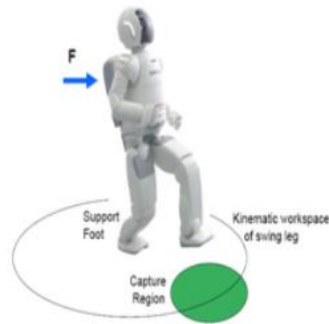


Figure 3.3: Capture Point [4]

In figure 3.3, the capture point is already defined by MPC as predicting the step in the future horizon in case it is needed while having an external force applied on the robot trunk. The capture point concept helps the robot to make the recovery step to balance itself from falling.

3.5 Inverted Pendulum on Cart

When the bipedal robot receives sudden external perturbations, it may risk falling on ground. It is very important then to keep in mind while balancing the robot during the walking gait or the standing state that there is a controller to make it stable against any external perturbations. In the pre-defined walking gait, the author has assumed that the robot will receive the sudden external perturbations from sides in the lateral directions to the pelvis only.

In this thesis paper, in order to cover all the balancing issues that the robot may face, such vibration caused by external perturbations on pelvis may be tackled. From the different models of pendulum that have been discussed in the literature review, one may focus on the force that disturbs the robot since that it is one of the main problems of balancing.

The author has chosen, after having conducted the needed research, to apply the inverted pendulum on cart model since that it is considered as a benchmark tool of dynamics and testing control techniques. Since that the assumption is that the CoM is existing in the pelvis part of the robot and that the legs are almost massless, it is

therefore important to control the balance of the robot to prevent the fall down on ground. The inverted pendulum is by nature an unstable nonlinear system.

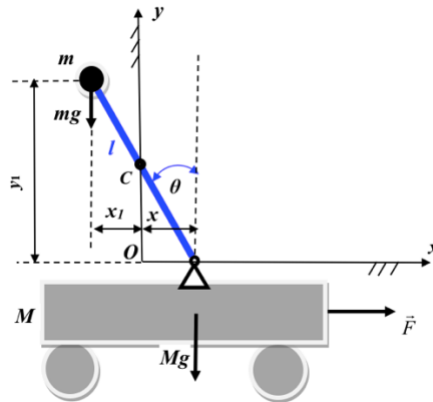


Figure 3.4: Inverted Pendulum on a Cart [19]

Figure 3.4 illustrates the model I will use in this part to tackle the vibration control.

The cart moves in a horizontal way in the x direction with a mass M , while the inverted pendulum right on top of the cart is attached to the cart with a massless rigid rod (Figure 3.4). The pendulum has a mass m and rod length l . The gravity forces are mg as for the pendulum and Mg as for the cart respectively, where g is the acceleration of gravity. It is assumed that there is no friction on ground. The external force F is applied to the cart in the x axis direction. The pendulum is rotating from the vertical by angle θ . It is important to understand the inverted pendulum in order to make it stable in the upright position.

Let us choose the fixed axes of coordinates x and y , assuming that the axis Oy passes through the initial position of the center of gravity C of the system (Figure 3.4).

The position of the system relative to the fixed axes xOy is determined by the coordinate of the center of gravity of the cart x and the angle of rotation of the pendulum θ relative to the vertical (Figure. 3.4). That is, the given system has two degrees of freedom.

Let's take the coordinate x and angle θ as generalized coordinates (Figure 3.4).

Then the dependence of the coordinates center of gravity of the inverted pendulum x_1 and y_1 on the generalized coordinates x and θ will have the form:

$$x_1 = x - l \cdot \sin\theta \quad (3.1)$$

$$y_1 = l \cdot \cos\theta \quad (3.2)$$

Looking to the velocity direction, it can be calculated as the first derivate of x_1 and y_1 in respect to time as:

$$\dot{x}_1 = \dot{x} - l \cdot \dot{\theta} \cdot \cos\theta \quad (3.3)$$

$$\dot{y}_1 = -l \cdot \dot{\theta} \cdot \sin\theta \quad (3.4)$$

So, in order to find the equation of motion, the derivation of the Lagrange's equations is based on kinetic energy and potential energy.

The potential energy of the pendulum is expressed as:

$$V = m \cdot g \cdot y_1 = m \cdot g \cdot l \cdot \cos\theta \quad (3.5)$$

The kinetic energy of the cart can be expressed as:

$$T_{cart} = \frac{1}{2} M \cdot v^2 = \frac{1}{2} M \cdot \dot{x}^2 \quad (3.6)$$

The kinetic energy of the pendulum is expressed as:

$$T_{pend} = \frac{1}{2} m \cdot v_1^2 = \frac{1}{2} m \cdot (\dot{x}_1^2 + \dot{y}_1^2) \quad (3.7)$$

The kinetic energy of the whole system is expressed as:

$$T = T_{cart} + T_{pend} = \frac{1}{2} M \cdot \dot{x}^2 + \frac{1}{2} m \cdot (\dot{x}_1^2 + \dot{y}_1^2) \quad (3.8)$$

Taking into account expressions (3.3) and (3.4), we obtain the kinetic energy of the entire system:

$$\begin{aligned} T &= \frac{1}{2} M \cdot \dot{x}^2 + \frac{1}{2} m \cdot (\dot{x}^2 - 2 \cdot l \cdot \dot{x} \cdot \dot{\theta} \cdot \cos\theta + l^2 \cdot \dot{\theta}^2 \cdot \cos^2\theta + l^2 \cdot \dot{\theta}^2 \cdot \sin^2\theta) \\ &= \frac{1}{2} (M + m) \cdot \dot{x}^2 - m \cdot l \cdot \dot{x} \cdot \dot{\theta} \cdot \cos\theta + \frac{1}{2} m \cdot l^2 \cdot \dot{\theta}^2 \end{aligned} \quad (3.9)$$

The kinetic (generalized) potential of the system will be:

$$L = T - V = \frac{1}{2} (M + m) \cdot \dot{x}^2 - m \cdot l \cdot \dot{x} \cdot \dot{\theta} \cdot \cos\theta + \frac{1}{2} m \cdot l^2 \cdot \dot{\theta}^2 - m \cdot g \cdot l \cdot \cos\theta \quad (3.10)$$

Lagrange's equations have the form:

$$\frac{d}{dt} \left(\frac{\partial L}{\partial \dot{x}} \right) - \left(\frac{\partial L}{\partial x} \right) = Q_x = F(t) \quad (3.11^*)$$

$$\frac{d}{dt} \left(\frac{\partial L}{\partial \dot{\theta}} \right) - \left(\frac{\partial L}{\partial \theta} \right) = Q_\theta = 0 \quad (3.11^{**})$$

Q_x and Q_θ are generalized forces which indicate the external forces at the generalized coordinates x and θ .

The first equation of motion will be in the x direction, and according to the Lagrange's equation (3.11^{*}), taking into account the kinetic (generalized) potential (3.10), we will get:

$$(M + m) \cdot \ddot{x} - m \cdot l \cdot \ddot{\theta} \cdot \cos\theta + m \cdot l \cdot \dot{\theta}^2 \cdot \sin\theta = F(t) \quad (3.12)$$

The second equation of motion will be according to the Lagrange's equation (3.11**), taking into account the kinetic (generalized) potential (3.10), we will have:

$$l \cdot \ddot{\theta} - \ddot{x} \cdot \cos\theta - g \cdot \sin\theta = 0 \quad (3.13)$$

After deriving the Lagrange's equations of motion, the next step is to derive the state space of the inverted pendulum on cart in order to get the matrices A and B that will be used as input in the linear quadratic regulator matrix calculations. By setting priorities to either the linear displacement of the cart, the velocity of the cart, the angular displacement of the pendulum or the angular velocity of the pendulum, the system shall control the vibration accordingly. In the section of simulating the linear quadratic regulator controller on the inverted pendulum on cart, further details shall be explained.

3.6 Proposed Vibration Control Controllers

3.6.1 Fuzzy Logic

The inverted pendulum on cart is an unstable and non-linear system. It has complex and multivariable nature of system. In this thesis paper, the author proposed to tackle the problem of the vibration caused by sudden external forces laterally on the pelvis which is the base of the inverted pendulum on cart. Authors in the literature papers have suggested and experimented different controllers in order to tackle the vibration and further control it. Roose et al. [20] in his paper used fuzzy logic with PID controller since that PID stabilizes only linear systems. He used fuzzy logic because it uses linguistic variables and their membership functions as rule-base to get the proper output. Roose et al. [20] concluded that the performance of the fuzzy logic controller for balancing the vibration of the inverted pendulum was successful in providing such better settling time and lowest overshoot. Abut et al. [21] in his paper defined fuzzy logic as it uses approximate thinking instead of thinking based on exact values which is suitable for systems with difficult mathematical model. Expert people who have knowledge about the system set the if-then set of rules in the rule base of fuzzy logic. He concluded from his experiment of the PID- type fuzzy that the system had the lowest amplitude while reaching stability position and best performance for settling time.

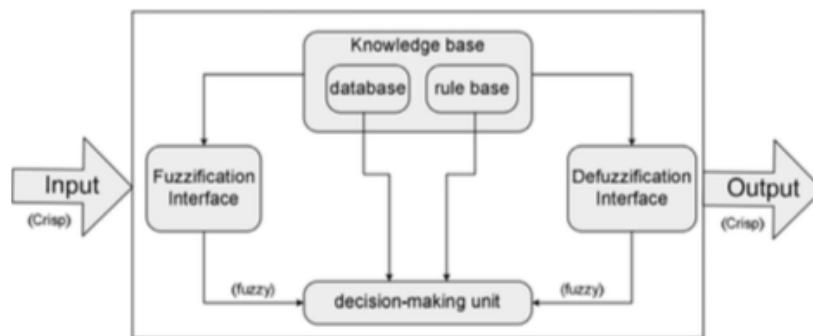


Figure 3.5: Fuzzy Logic Model Concept [20]

Figure 3.5 explains the block diagram of the fuzzy logic model concept of knowledge base of set of rules done by the process engineer. There are fuzzification and defuzzification processes while checking the decision-making unit in order to make the minimal error.

3.6.2 Linear Quadratic Regulator

Another solution for controlling such vibration applied on the base of the inverted pendulum on cart is the linear quadratic regulator. The LQR optimizes the cost function in a system when it is in a nonlinear state. It is used as a state feedback gain. Unlike the PIDs, the LQR studies the system behavior through the state space form. Using trial and error, a process engineer should tune the linear quadratic regulator matrices Q and R which are the state weighting matrix and control weighting matrix respectively in order to get the optimal control over the external perturbations and minimize the overshooting and settling time. Marada et al. [22] experimented the linear quadratic regulator using genetic algorithm and he found that the matrices Q and R are easily optimized. He also concluded in his paper that the linear quadratic regulator successfully controlled the external perturbation applied on the inverted pendulum with one small overshoot in the case of no input disturbance and few small overshoots with input disturbance. By applying genetic algorithm with LQR, Marada could get robustness and effectiveness for the system. Fauziyah et al. [23] in her paper also tried the combination of LQR with pole placement as experiment in which she concluded that both combined can produce optimal system of response and minimal control signals. This controller is further explained in the modelling section since that it is decided to use it as for controlling the inverted pendulum on cart model against the external perturbations.

3.6.3 Fuzzy Linear Quadratic Regulator

Fuzzy linear quadratic regulator is a combination of fuzzy logic with linear quadratic regulator controller. It has a better performance and robustness compared with both controllers separately. Recent literatures have shown better results based on this model. Hazem et al. [24] with his group have proven in their paper that this model has improved the settling time, the peak overshoot, steady state error and the total root mean square error by high percentage when they applied this model on double inverted pendulum. this model shall be in the future works as a continuation to the optimization of vibration control to the system against sudden external perturbations.

3.7 ZMP for Dynamic Balance

It is essential to balance the bipedal robot dynamically while walking or standing. Such a strategy must exist in order to prevent the robot from falling on ground whether when it is in the double support phase or even single support phase. Literature authors have all agreed that in order to keep the robot dynamically balanced one should concentrate on ZMP in the support polygon. Bahdi et al. [4] illustrated how the robot NAO was dynamically balanced by making ZMP in the support polygon. Dehart et al. [14] illustrated the importance of the ZMP at which the robot remains stable. Al-Shuka et al. [8] built his dynamic balance strategy based on ZMP. Thus, it is crucial to keep the ZMP in the support polygon around the center of pressure so that the walking robot remains stable. In the next chapter, the application of the controller for the ZMP shall be further illustrated into how to keep it in support polygon during the gait.

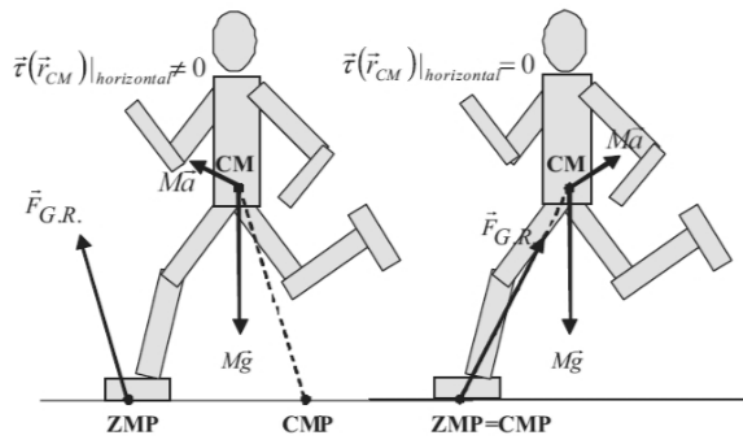


Figure 3.6: ZMP for Dynamic stability [14]

Figure 3.6 shows how important it is to keep the ZMP in the support polygon around the foot in order to keep the dynamic balance of the robot.

3.8 CoM for Static Balance

The bipedal robot on the other hand should remain statically balanced. The universal method of keeping the robot statically balanced is by keeping the GCoM in the support polygon. This is generally done through ankle and hip of the robot. Jing et al. [25] successfully simulated his robot and made it statically stable by keeping the GCoM in the support polygon. Ding et al. [26] developed a nonlinear MPC in order to keep the

CoM in the support polygon. In the next chapter, further explanations shall take place into how the model was designed to keep the GCoM in the support polygon in the simulation to keep the robot statically balanced.

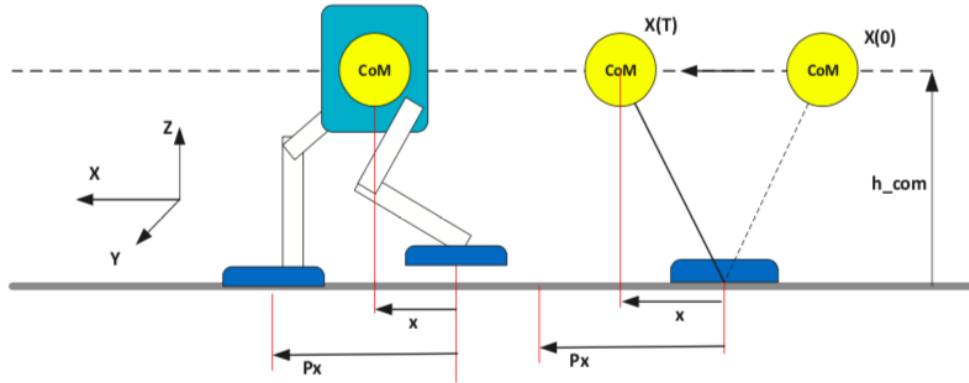


Figure 3.7: Center of Mass diagram [14]

Figure 3.7 illustrates how important is to calculate the center of mass in order to ensure the static balance of the robot.

3.9 Model Predictive Control

Model predictive control is based on anticipating the future motion steps over a future horizon. Aftab et al. [27] used this model predictive control scheme in his paper as a combination of ankle, hip and stepping strategy in order to obtain a human like walk. He used this scheme to generate future steps and keep the system balanced. He successfully maintained the balance against the perturbations using MPC. Araffa et al. [19] used MPC to generate CoM and ZMP trajectory for the future steps to maintain the stability with good accuracy results for his cart-table model. Shafiee-Ashtiani et al. [18] controlled the capture point in the desired position by employing MPC scheme through modulating ZMP and CMP. His purpose was to maintain the capture point, the CMP and the CoP in the center of the support polygon to keep his bipedal robot dealing with severe pushes. In the next chapter of modeling, the MPC controller shall be explained into deeper details about how it maintains the dynamic and static balance of the bipedal robot.

4. DESIGN AND MODELING

4.1 Software Used

The author has decided to use SOLIDWORKS and MATLAB kit since that they can be both integrated together to make further analysis. SOLIDWORKS was a good choice because in the occasion of problem occurrence with the design, one could change it at any point of design process whenever it is needed. Its tools help to have simple and quick designs as well as 360 view to the design details to make sure it could work before being manufactured. MATLAB is important because of its powerful library for coding and controllers design and furtherly importing the CAD design to analyze it and get its data on graphs.

4.2 Bipedal Robot Design

4.2.1 Initial Design

In a previous Mechatronics Master's program course, the author has tried to design and develop a physical skeleton of a raptor dinosaur that could walk with bipedal movement. The prototype skeleton was done by cardboard 4mm thickness (Figure 4.1). The microcontrollers used were Arduino UNO and Arduino MEGA. Sensors that were used are Ultrasonic, PIR and other different sensors for different tasks. The prototype skeleton also had motors for every joint that make it possible to move. The prototype succeeded to make a smooth movement like a real animal while having both legs moving simultaneously. However, the problem faced was that there was latency in responses to movement according to the sensors output as well as the mass distribution problem and the material used from which the raptor could make maximum 6 moves and then falls. Thus, the skeleton lacks the balance to keep moving without falling, under any circumstances of the ground type whether grass or bricks or asphalt or snow.



Figure 4.1: Initial skeleton design of the raptor dinosaur made with cardboard 4mm

4.2.2 Final 3D Design

In this section, the skeleton design process shall be shown. First, the author tried to modify the skeleton design on SOLIDWORKS software with full details of raptor dinosaur bone structure skeleton (Figure 4.2).

However, for mathematical reasons as well as the priority is given to proof of concept to the balancing methodology that is being followed in this thesis paper, the design had to be simplified. Due to the complexity of the mass distribution of the upper body of the skeleton, the upper body part total mass was assumed as concentrated in the pelvis. Thus, the head, tail and ribs have been removed and all the mass was considered to be in the pelvis only. The biological bone structure of the raptor dinosaur was further checked; and, some parts were modified to make it less complex in order to simplify the calculations during the balancing process.



Figure 4.2: The final 3D design of the raptor dinosaur

In Figure 4.2, the 3D design was simplified to pelvis and legs only to make calculations easier. The feet of skeleton have been modified and had their surface bigger so that the support polygon covers more area for balancing reasons.

4.2.3 Design Details

Below is the dimensions figure details of the raptor dinosaur pelvis and legs (Figure 4.3). The robot skeleton was almost designed close to the real bone structure of the real raptor with exceptions of foot design for a bigger support polygon in order to maintain balance during the simulation. The dimensions of the skeleton parts had to be close and proportional to keep the balance. The pelvis is 72 mm while the thigh is 63 mm and the calf is 65 mm respectively ending with the exceptional foot dimension which is 40 mm.

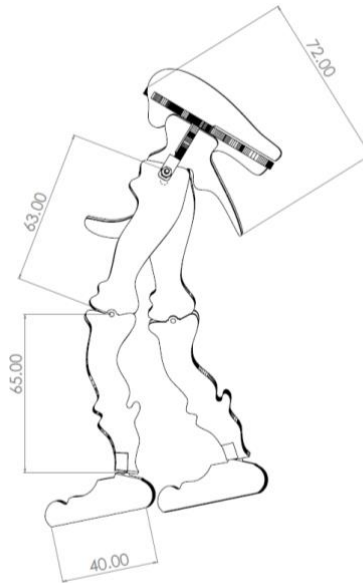


Figure 4.3: The raptor dinosaur main dimensions

Going deeper into the robot design details, the number of joints per each leg was determined according to the majority of literature papers suggestions. The legs are similar to the real raptor legs in the sense of the hip joint having 3 degrees of freedom, the knee with a single degree of freedom; while, the ankle has two degrees of freedom to seem similar to the real animal while smoothly moving in the simulation. So, the total per each leg is 6 DOF and total number of DOF's of the whole robot is 12 (Figure 4.4).

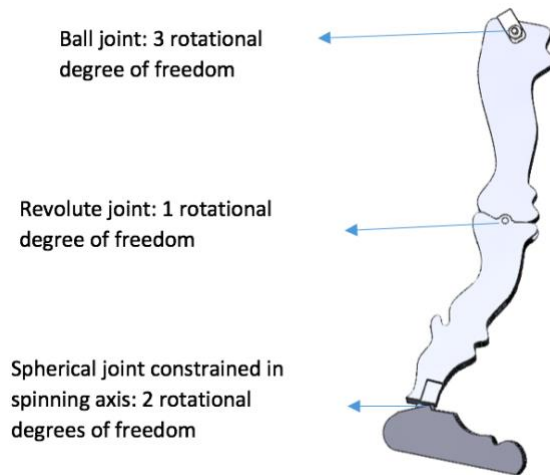


Figure 4.4: Leg DOFs details

Figures 4.5 and 4.6 are the details of how the leg’s parts are connected. The pelvis is connected to the hip by a ball joint (Figure 4.5). This ball joint is bolted to a bracket. There are 2 spacers in the hip joint to constrain the hip in the axial movement direction.

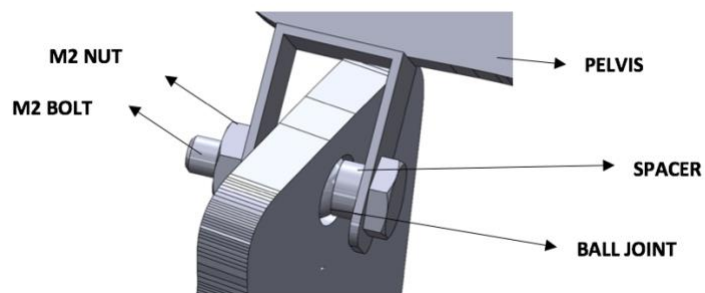


Figure 4.5: Pelvis and Hip Connection

The calf is connected to the hip through a revolute joint pin as shown in Figure 4.6.

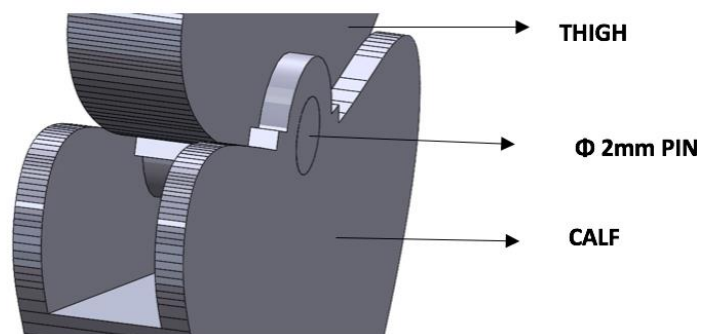


Figure 4.6: Hip and Calf connection

Finally, Figure 4.7 shows the connection between the calf joint and the foot. The calf is connected to the foot with a spherical joint. This spherical joint constraint prevents the spin axis rotation.

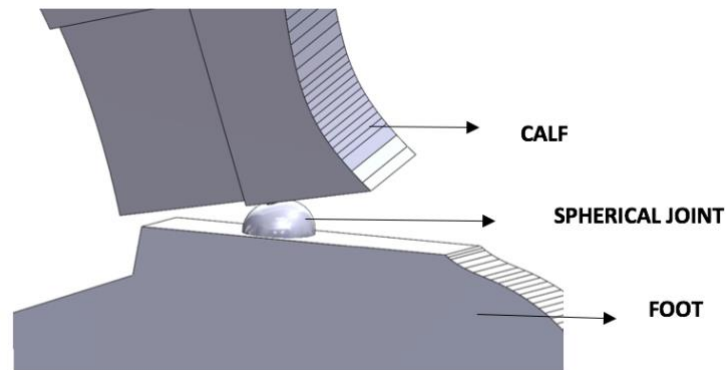


Figure 4.7:Calf and Foot connection

4.3 Modeling

4.3.1 Dynamic and Static Model

In this section, the models that were designed on MATLAB shall be illustrated as how to ensure that the balance is done dynamically and statically to the robot while walking. It is important to model the controllers to keep the gait as much as possible balanced while walking in the simulation. The designed robot was imported to the MATLAB and further blocks of controllers and mathematics were used from MATHWORKS library in order to control the locomotion of the bipedal robot movement as it is shown in Figure 4.8.

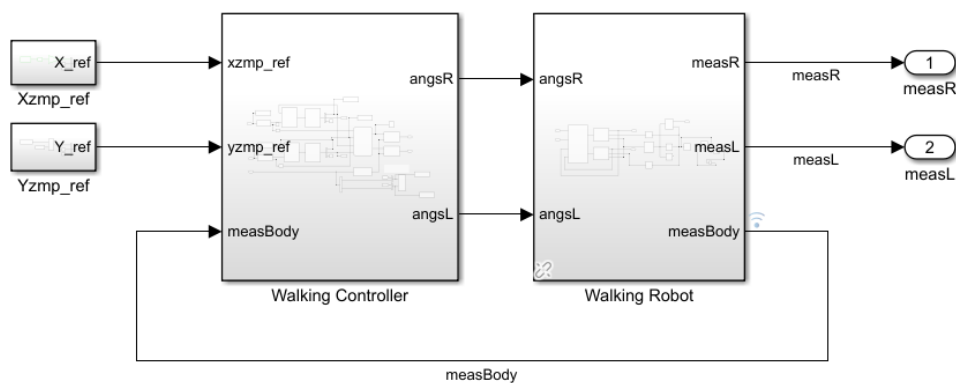


Figure 4.8:Dynamic and Static Balance Model

As it was mentioned in the previous chapter, in order to control the walking gait of the bipedal robot, the author has decided to control it dynamically using ZMP concept and statically using CoM concept. It is crucial to keep both in the support polygon while being in single support phase in order to maintain the robot stability; otherwise, the robot falls down on the ground.

Starting by the designed model, the author had to make it calculate the reference of the ZMP every step the robot makes and the GCoM as figure 4.8 shows. In order to keep control of these two important concepts, based on the literature results the model predictive control was used. Model predictive control anticipates the future stepping in a future horizon. Thus, it was important to put in the model MPC in order to anticipate and tell the robot to make the proper desired steps in order to keep the ZMP and CoM in the support polygon and further guarantee the future stability.

Going from left to right, the author had to firstly determine the xZMP reference for the system which is considered as the step planning. This step planning is defining the step length, timing(velocity) and the height of the step as shown in figure 4.8. The yZMP defines the foot lateral movement which is the step width. Both values go the walking controller block as the xZMP reference and yZMP reference in order to keep control of the dynamic walking gait of the robot.

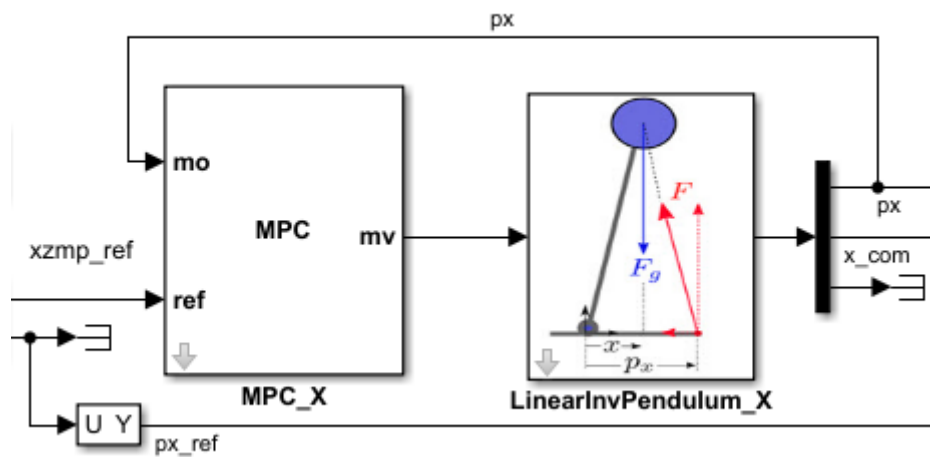


Figure 4.9: Walking Controller Subsystem

Figure 4.9 illustrates more the walking controller block. Inside of the block there is model predictive control in order to anticipate the future steps in the future horizon and keep the system informed of which step should be taken to guarantee the dynamic and static balance. The MPC block receives the xZMP reference and the current measured output signal as (mo). The block computes the optimal manipulated variable (mv) by

solving a quadratic programming problem. The manipulated variable is sent as an input to the inverted pendulum block in order to calculate the xCoM location and velocity. The block of the inverted pendulum gets output of xZMP and xCoM as outputs. The xZMP goes back to the MPC block as updated measured output and the xCoM is sent to the stepping logic block to take a step. Similar subsystem was done for yZMP and yCoM in another controller block. In the next chapter of simulation, the stepping methodology shall be illustrated in details in order to make the robot make a step while keeping its dynamic and static balance.

4.3.2 Vibration Control Model

While being in the walking gait, the bipedal robot may receive external disturbance or perturbations that may affect the balance and make it fall on ground. This external disturbance can be in terms of external force applied to the skeleton. The author has assumed in the pre-defined walking gait section that the simulation for this part will be on external perturbations applied on the pelvis. The inverted pendulum on cart model was used as the model (subparagraph 3.5) on which the vibration applied on pelvis shall be controlled. In this case, the author has made a model using the LQR controller. The LQR controller in the literature results have proven its robustness and effectiveness in stabilizing the system.

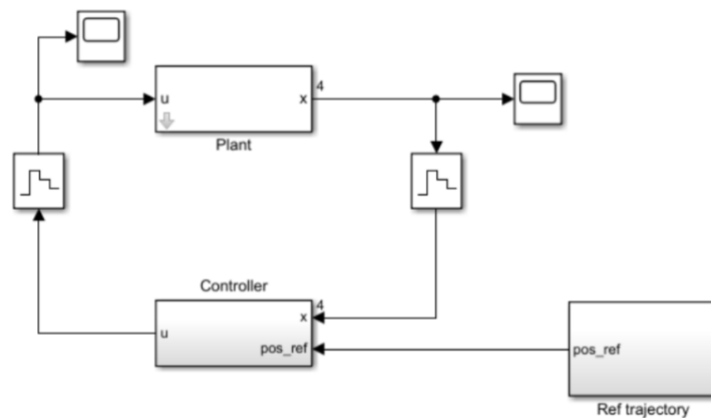


Figure 4.10: vibration control using LQR model

Figure 4.10 illustrates the vibration control model using LQR controller. In the Ref Trajectory block the author has identified the position reference of the cart of the inverted pendulum.

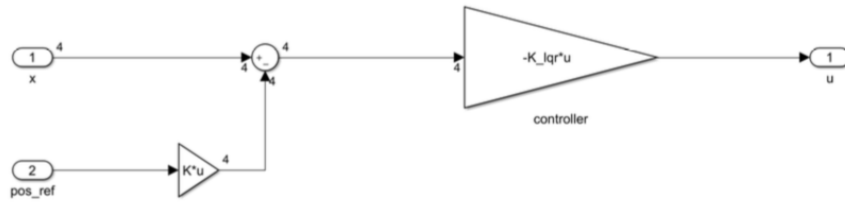


Figure 4.11:LQR Controller

The cart reference position along with the state vector x are passed as input to the controller block and then passed to the summation block then forwarded to the LQR controller in order to get the output which is the control input u as shown in Figure 4.11.

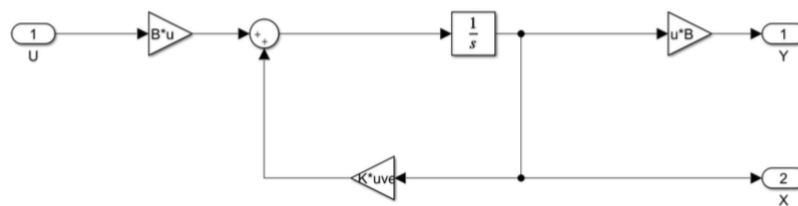


Figure 4.12:Plant Block

The control input u is afterwards passed to the plant block as shown in Figure 4.12. It is multiplied by the matrix B while x is multiplied by matrix A . Both sides are sent to the summation block from which state space is constructed. Then, x derived again from the equation to pass to the controller again. In the next chapter of simulation, it shall be illustrated more how the calculations are made in this model in order to control the cart displacement and pendulum angle.

5. SIMULATION AND ANALYSIS RESULTS

5.1 Dynamic and Static Balance Simulation

The author designed the bipedal robot on SOLIDWORKS. The bipedal robot in the simulation consists of pelvis and 2 legs. The dimensions are set as described in the previous section of design. The author has imported the design to MATLAB in order to apply the pre-defined walking gait that have been previously set. Regarding the dynamic balance, the author concentrated on keeping the ZMP in the support polygon using the model predictive controller.

Table 5.1 The dimensions of the designed robot

| Part | Length(mm) |
|-------------|-------------------|
| Pelvis | 72 |
| Hip | 63 |
| Calf | 65 |
| Foot | 40 |

As Table 5.1 shows, these are the dimensions of the robot parts. They were proportionally with these dimensions to make sure that the robot can be balanced in the simulation. The surface of the foot was big enough to make sure that the support polygon around the feet is quite big while experimenting the ZMP and CoM.

The pelvis was set with a density of 500 kg/m^3 . Regarding the pre-defined walking gait, the author assumed that the walking gait will be in a straight line. Table 5.2 shows the walking gait description.

Table 5.2 The walking Pre-definition

| Walking Steps | Simulation Period (s) | Pelvis Density (kg/m^3) |
|----------------------|------------------------------|--|
| 28 | 15 | 500 |

In the beginning of the walking gait, the robot adjusts his standing before it starts stepping. It takes 0.8 seconds to adjust his joints angles. Table 5.3 shows the initial angles of the different joints of the standing robot during the double support phase before it starts stepping.

Table 5.3 Joints angles during the double support phase

| Joint | Initial Standing Double Support Phase Angle (rad) | Stepping Single Support Phase Angle (rad) |
|--------------|--|--|
| Hip Pitch | -0.45 | -0.1 |
| Hip Roll | 0 | 0.25 |
| Knee Pitch | 0.91 | 1.1 |
| Ankle Pitch | -0.45 | -0.52 |
| Ankle Roll | 0 | 0.05 |

In Table 5.3, it is shown the initial angles to make the robot initially stable in the double support phase before making the steps. In the stepping phase where the robot is being in the single support phase such angles were provided in table 5.3 when the leg is stretched at the maximum before it places the foot on the ground.

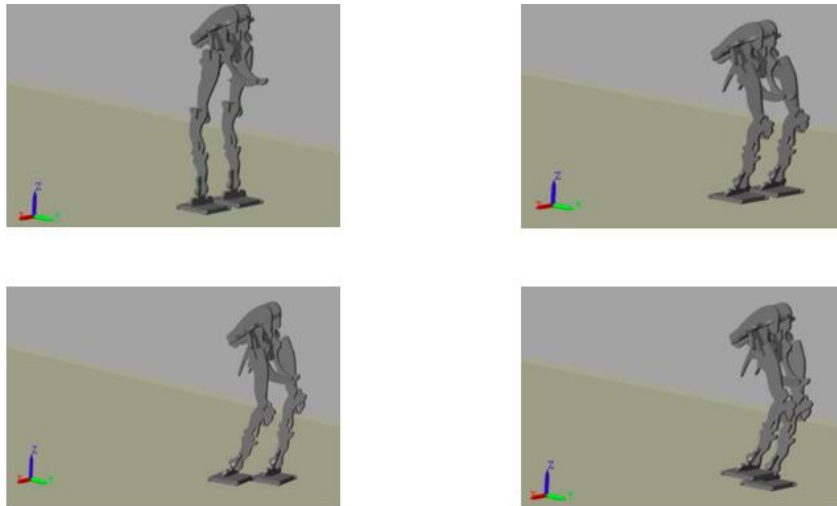


Figure 5.1: Movement frames

As it is shown in Figure 5.1, these are the frames of movement of the robot in the simulation. The robot in the beginning is standing straight, then he adjusts the initial angles for the hip, knee and ankle joints during the double support phase. The robot afterwards starts stepping and going to the single support phase by lifting the leg up and move forward to make a step then the other leg does the following step.



Figure 5.2: the balancing factors

Technically speaking, during the walking gait, the robot had to maintain during the single support phase the ZMP in the support polygon of the stance leg which supporting the whole weight of the pelvis in order to keep it dynamically stable. The ZMP was around the center of pressure in the support polygon in the different steps during the walking gait because of the control of the model predictive controller that was keeping the steps in the right positions as desired by the controller while comparing to the reference positions of $xZMP$ and $yZMP$. This controller was at the same time controlling the $xCoM$ and $yCoM$ which are the trajectories of center of mass in the pelvis as ground projections in the support polygon to keep the robot statically stable (Figure 5.2).

Looking deeper into the dynamic and static balance model explained in the previous chapter, the $xCoM$, $yCoM$ along with the $xZMP$ reference for the step-forward and $yZMP$ reference for the step-lateral were sent from the controller to the stepping logic block in order to inform the system with the desired steps that the right leg and left leg should make in the future motions as shown in Figure 5.3.

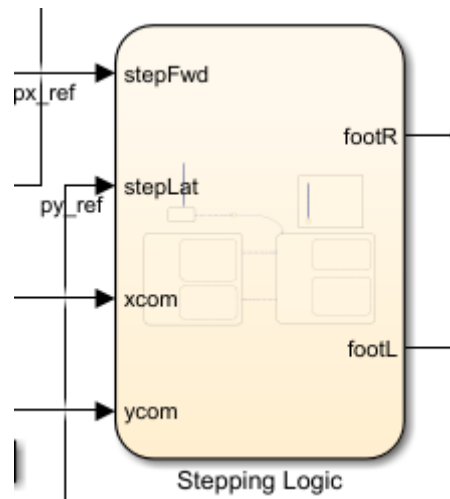


Figure 5.3: stepping logic block

For each foot, the foot desired position set by the stepping logic along with the calculated altitude were sent to inverse kinematics block in order to get the correct joints' angles for each leg to ensure the balance of the robot after making the future desired step.

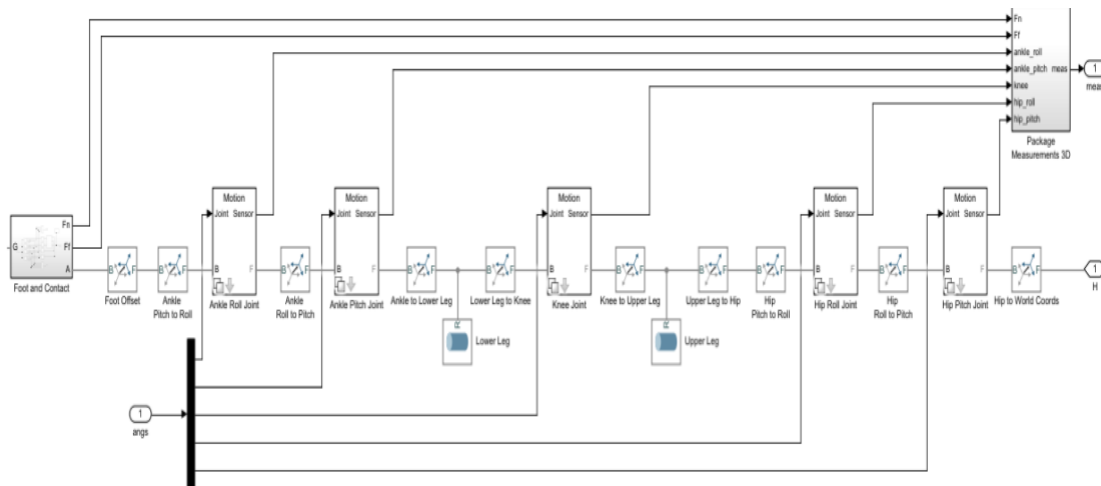


Figure 5.4: The multibody model

As shown in Figure 5.4, The desired angles are then sent to this multibody block in which all angles are sent to the different hips, knees and ankles joints in order to make the proper future step desired by the system. Afterwards, the measured joints are sent back to the controller block in order to re-calculate again the future steps based on the actual calculated one.

The robot understands in the simulation that it is touching the ground through the force sensors. There are 4 force sensors on each foot since that it is important during the single support phase.

5.2 Dynamic and Static Balance Results

In the analysis of the motion, the author has tested the robot walking gait in the 15 seconds of motion in the straight direction for 28 steps of walk. For the dynamic balance, the actual xZMP, which is the step length and timing(velocity) and height of the step, was tested and compared with the reference xZMP in order to check if the robot is balanced dynamically or not.

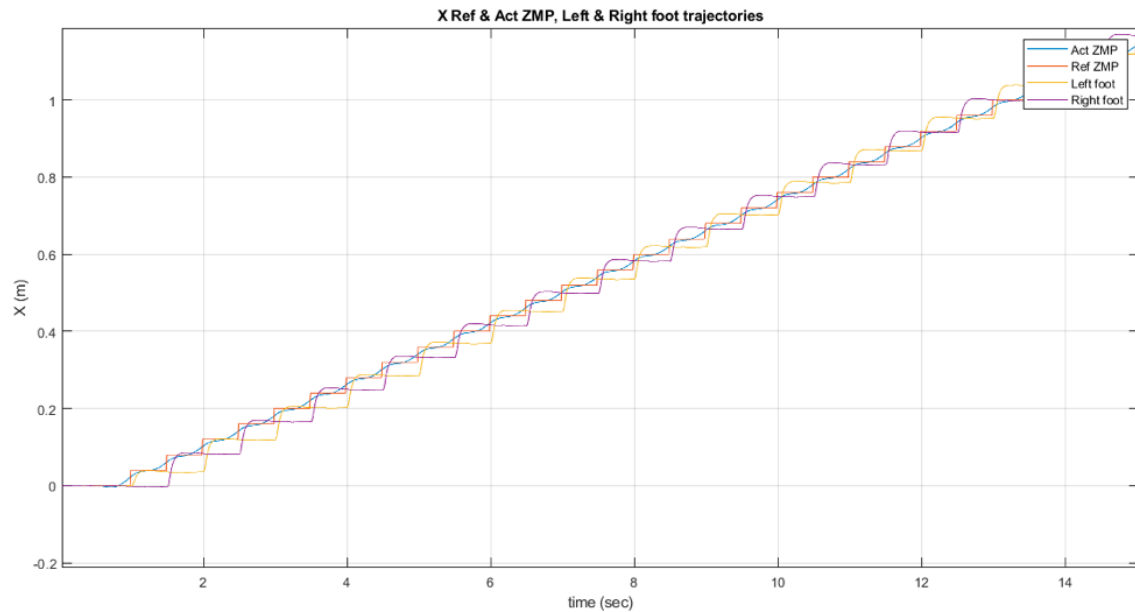


Figure 5.5: Actual xZMP vs. Time

As it is shown in Figure 5.5, the actual xZMP was close to the reference xZMP. The Figure 5.5 shows the placement of right foot and left foot during the walking gait. The desired xZMP must be in the support polygon of the foot that is on the ground and carrying the whole weight of the pelvis. In order to have the dynamic balance stable the xZMP should be existing in the foot that is placed on ground. According to the graph and simulation results, the actual xZMP was close to the reference xZMP which is controlled by the model predictive controller that anticipates the future steps and controls the desired xZMP positions. Test result is that the robot is dynamically balanced in the step forward for the 28 foot-steps done by both feet in 14.2 seconds of actual SSP gait.

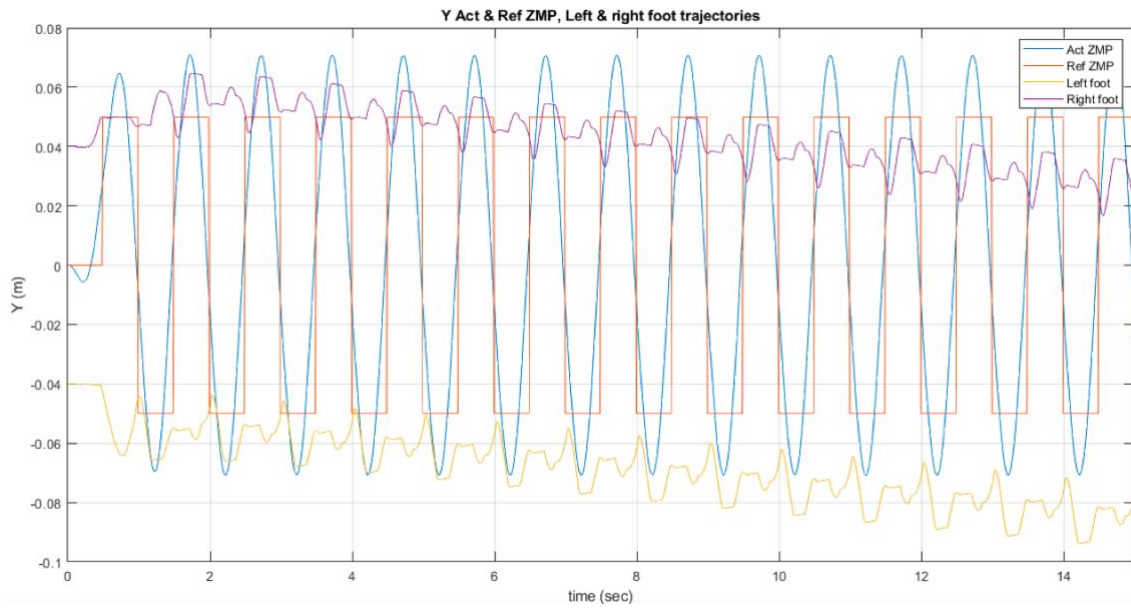


Figure 5.6: yZMP vs. Time

The second test for the dynamic balance was to investigate the actual yZMP position compared with the reference yZMP which is responsible for the lateral step of the robot. As shown in Figure 5.6, test result graph shows that the actual yZMP was in the same direction of the reference desired yZMP which was controlled by the model predictive controller. The actual yZMP was existing in the same direction of where the reference must be which the direction of the actual foot placed on ground. As it is shown in Figure 5.6, when the signal of the foot placement goes to the peak, the reference yZMP is desired to be in the same direction and successfully the actual yZMP was in the same direction. Test result for the actual yZMP which is responsible for the lateral step and a part of the dynamic balance was successful.

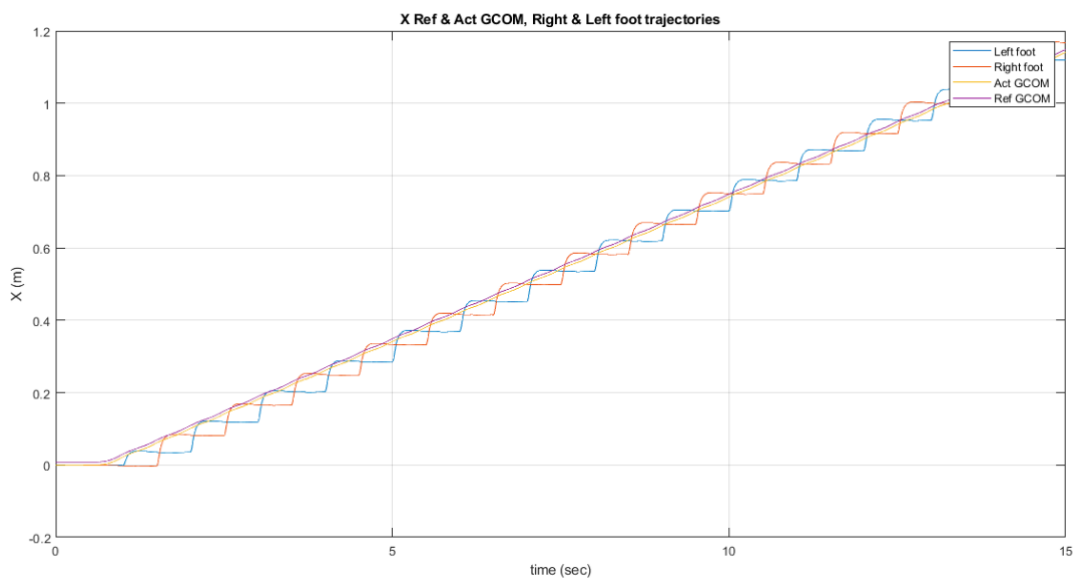


Figure 5.7: xCoM vs. Time

Regarding the static balance of the walking gait robot, as Figure 5.7 shows, it was tested how the GCoM existed in the support polygon in order to maintain the static balance. The walking gait of the robot was tested in the 28 walking steps with a time of 15 seconds of how the GCoM in pelvis existed in the center of the support polygon. As Figure 5.7 shows, the xCoM that was calculated by the model predictive controller for the desired future steps was compared with the actual position of the GCoM. In the graph also there are both feet placements to check how statically the robot was balanced. As it is shown, during the entire walking gait, the actual xCoM was aligned to the desired xCoM that was referenced by the controller. In the simulation, the robot was statically balanced in the 28 walking gait steps (SSP) without any fall on ground. Test result is that the robot was statically balanced during the 15 seconds of walking gait.

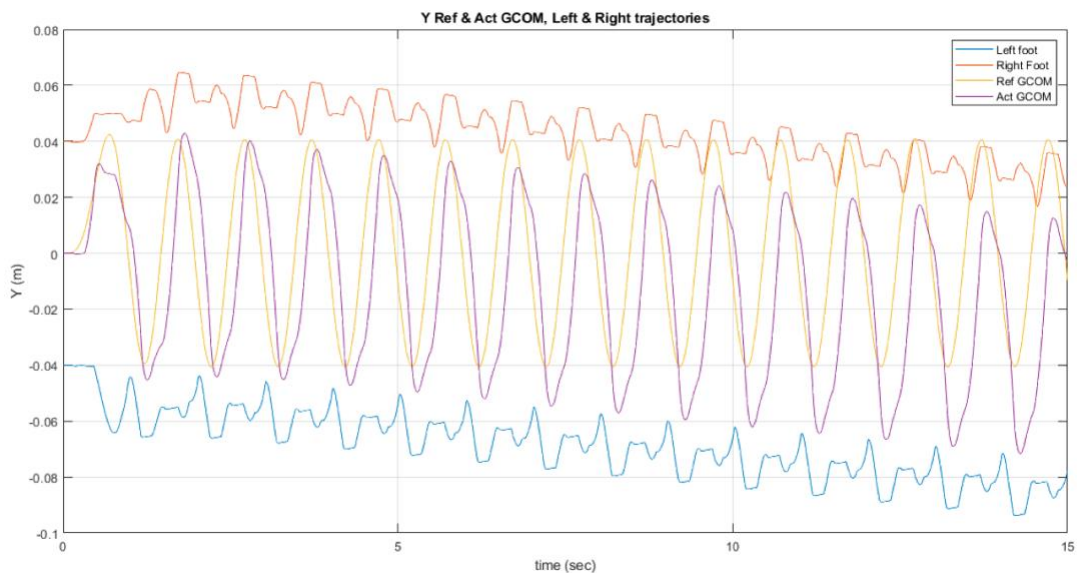


Figure 5.8: yCoM vs. Time

In the second test of the static balance of the robot, as Figure 5.8 shows, the author has tested the actual yCoM with the reference yCoM that is desired by the model predictive controller. As it is shown in the graph, the actual yCoM was almost the same as the desired reference yCoM. The reference yCoM tends to be close to the foot that is on the ground in order to maintain the robot statically balanced from the lateral direction. Test result graph shows successful position of the actual yCoM and thus the robot was balanced statically during the whole walking gait in the 28 footsteps.

Additionally, further analysis and tests were conducted regarding the walking trajectory of the robot on how the joints responded to the movement through dynamic time response analysis.

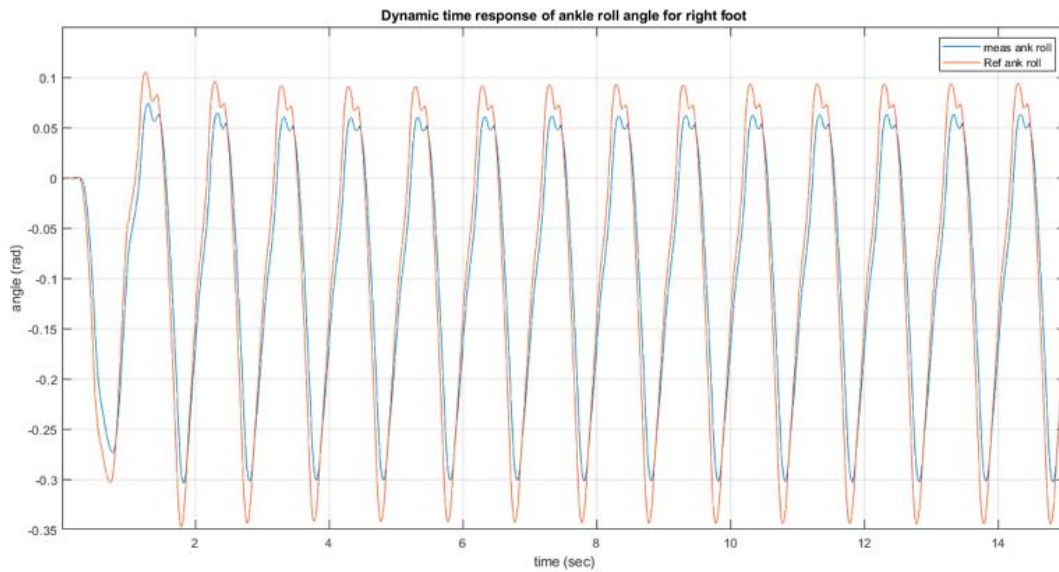


Figure 5.9: Ankle roll Dynamic times response

As it is shown in the Figure 5.9, the measured angle of the ankle roll joint followed exactly the reference ankle roll in terms of time with almost no delay. However, there was a slight difference of angle degrees error of average 1.7 degrees. Same dynamic time response was for the ankle pitch angle and the analysis shows that there was almost no time delay; instead, there was a slight angle error of 0.06 degrees on average as it is shown in the next figure 5.10.

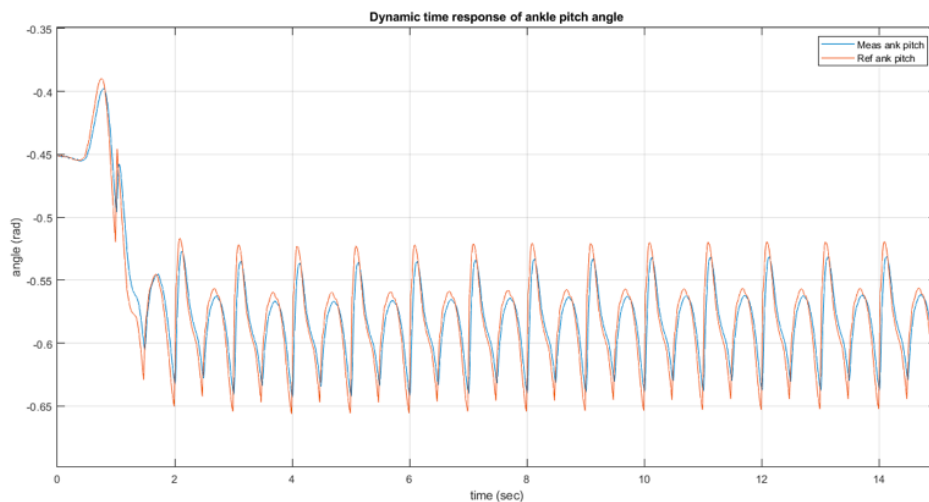


Figure 5.10: ankle pitch dynamic time response

Same analysis was applied as well on the knee joint as it is shown in the following Figure 5.11 results.

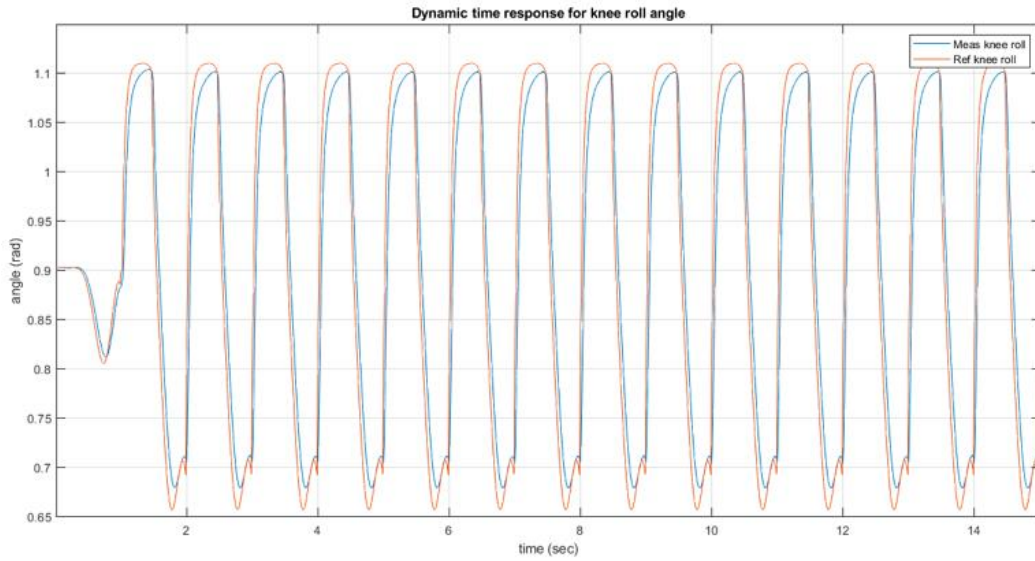


Figure 5.11: knee roll dynamic times response

In Figure 5.11, regarding the knee roll joint, there was almost no time delay however, there was a slight difference of degrees on average 0.13 degrees.

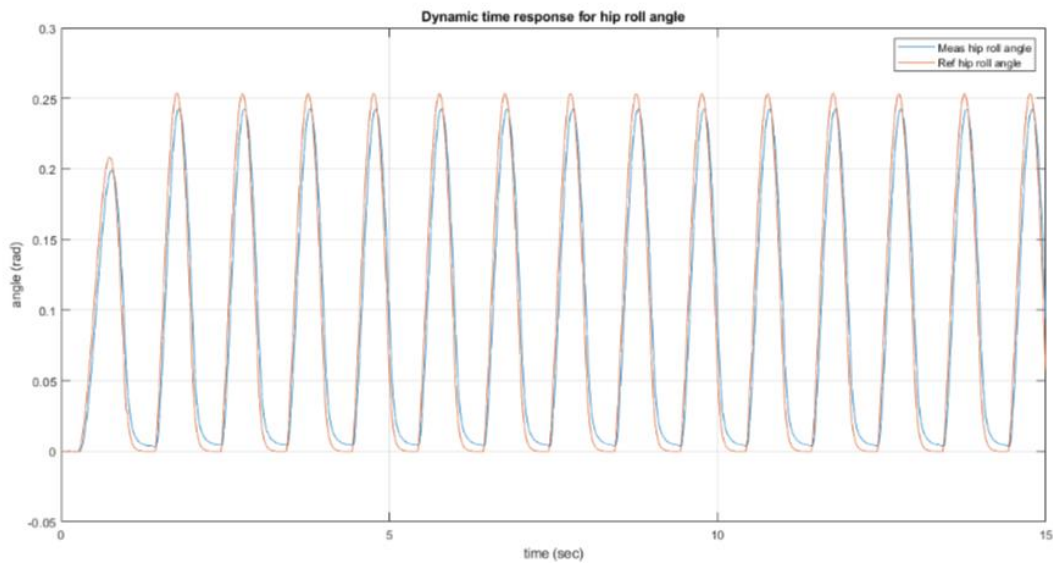


Figure 5.12: Hip roll dynamic time response

The hip roll and pitch angle dynamic times response were analyzed and there was almost no time delay as shown in figures 5.12 and 5.13. However, there was for the hip roll (Figure 5.12) an error of 0.1 degrees on average and for the hip pitch angle a slight difference of 0.11 degrees on average as error between the measured and the reference angles as Figure 5.13 shows.

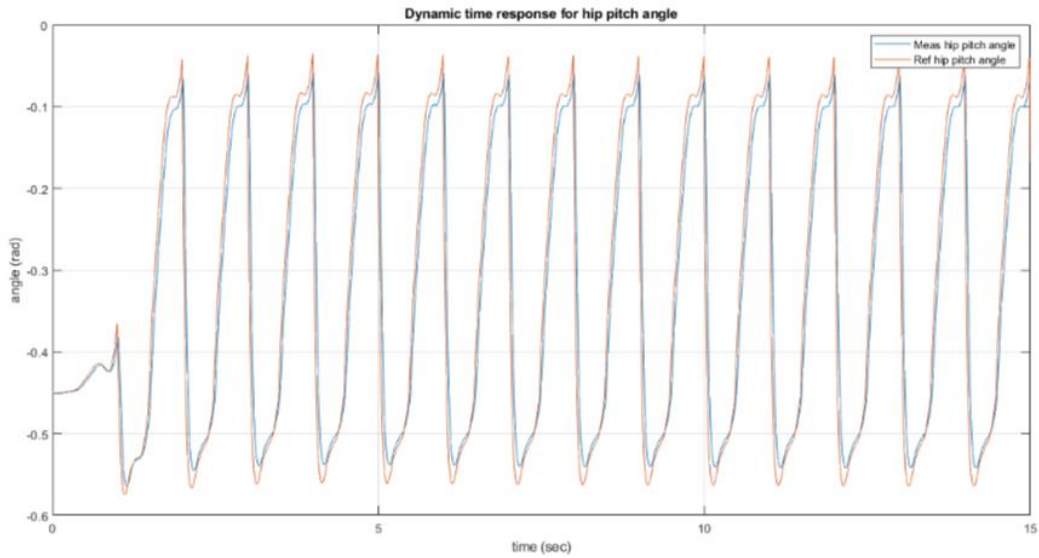


Figure 5.13: hip pitch dynamic times response

5.3 Vibration Control Simulation

After deriving the equation of motion of the inverted pendulum on cart and linearizing it, it is needed to get the state space which is expressed as follows [23]:

$$\dot{x} = Ax + Bu \quad (5.1)$$

$$y = Cx + Du \quad (5.2)$$

x is a vector state, u is a control input which is the force, A is a system matrix, B is input matrix, C is an output matrix and y is an output vector.

The linear quadratic regulator I used in the model in order to control the inverted pendulum on cart is depending on Q and R weight matrices to get the most optimal response with a purpose of regulating the system to make the output y be zero with minimum input. The LQR feedback the full state vector, which is x derived from state space in the equation 5.1 and multiplies it by the matrix gain K and subtract it from the scaled reference gain in order to get the optimal output. The purpose is to the optimal K by choosing the optimal characteristics through performance and effort which Q and R .

The LQR problem is as follows [23]:

$$j = \int_0^{\infty} [x^T(t)Qx(t) + u^T(t)Ru(t)] \quad (5.3)$$

Q is the performance weight matrix and R is the energy control.

And, the feedback control law that can minimize the value of cost is [23]:

$$u = -Kx \quad (5.4)$$

The optimal gain of feedback K can be expressed as [23]:

$$K = R^{-1}B^T P \quad (5.5)$$

P is found by solving Riccati equation by [23]:

$$A^T P + PA - PBR^{-1}B^T P + Q = 0 \quad (5.6)$$

In the inverted pendulum vibration control simulation, the author had to make trial and error in order to find the optimal control to the system while receiving external perturbation. In the simulation, the author had to compromise between the performance Q and the actuator effort which is R in order to have the optimal gain K. In that case, the author gave equal priority to linear displacement of the cart q_1 , same as the velocity of the cart which is \dot{q}_1 , same as the angular displacement link which is q_2 , same as angular velocity of the link which is \dot{q}_2 . So, the author had to penalize all these important factors the same way in the matrix giving them the same priority.

5.4 Vibration Control Analysis Results

In order to get the optimal result for vibration control, the author had penalized all the q's the same by creating an identity matrix called eye. This matrix made cart displacement, velocity, the link angular displacement and velocity as same priority. The mass of the cart was set as 1.5 kg, the mass of the pendulum as 0.5 kg and the length of the rod as 1 meter. Table 5.4 shows the different gains k's after making the command of the $k=lqr[A,B,Q,R]$.

Table 5.4 K parameters while changing Q and R scales

| No | K1 | K2 | K3 | K4 | Q | R |
|----|--------|--------|--------|-------|--------|----|
| 1 | -14.14 | 171.88 | -25.27 | 54.75 | 1*eye | 1 |
| 2 | -0.99 | 53.46 | -2.81 | 15.38 | 1*eye | 1 |
| 3 | -1 | 53.46 | -2.81 | 15.38 | 10*eye | 10 |
| 4 | -1 | 53.46 | -2.81 | 15.38 | 10*eye | 10 |

The identity matrix (eye) set is as $\begin{bmatrix} 1 & 0 & 0 & 0 \\ 0 & 1 & 0 & 0 \\ 0 & 0 & 1 & 0 \\ 0 & 0 & 0 & 1 \end{bmatrix}$.

The author has multiplied the identity matrix with a scale of 1 and 10 as a trial and error to get the best gain k 's in order to minimize the peak overshoot and settling time of the curve. The author has tried the simulations with R matrix as 1 and 10.

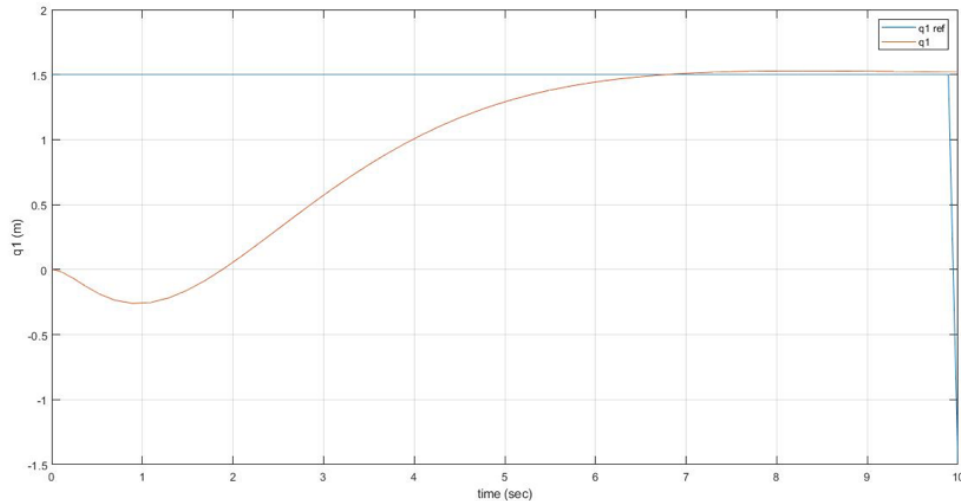


Figure 5.14: cart linear displacement vs. time

As a result, the optimal control for the cart linear displacement was as shown in Figure 5.14. It has a small peak overshoot and the time the cart took to settle and stabilize was 6.7 seconds.

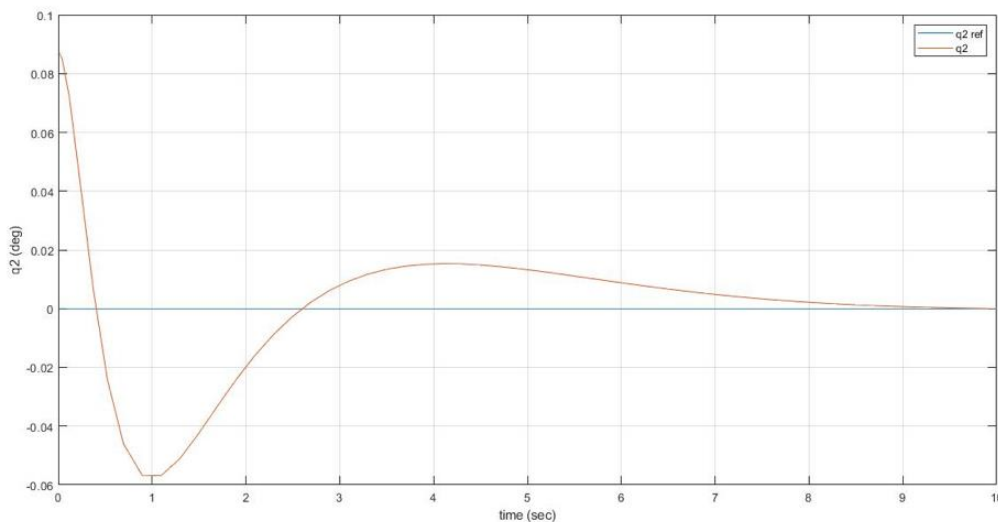


Figure 5.15: Link angular displacement vs. time

As a result, the optimal control to make the link of the pendulum angular displacement go back to zero was 9.3 seconds as Figure 5.15 shows.

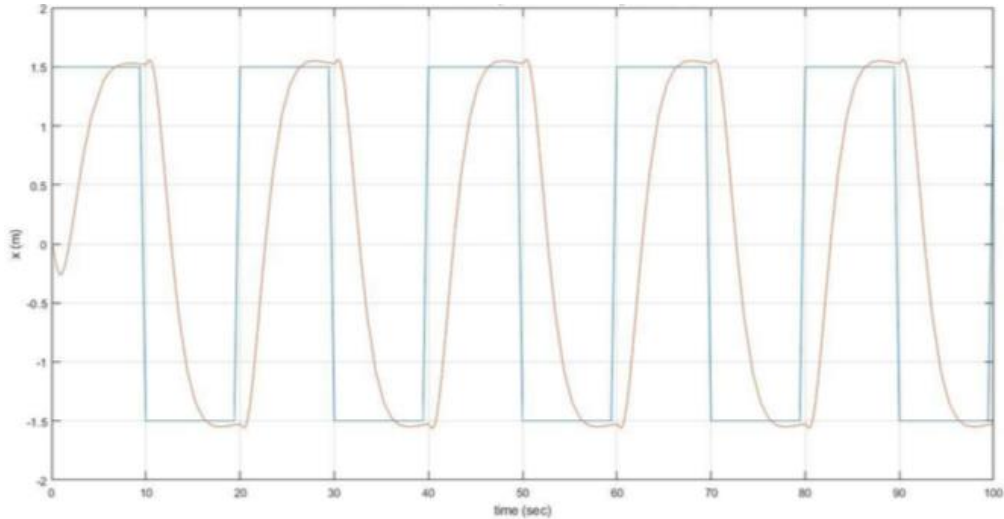


Figure 5.16: cyclic external disturbance control graph for q_1

The simulation was extended to make cyclic external disturbance every 10 seconds to see how the LQR controller will respond and the result was found the same as Figure 5.16 shows. It takes 6.7 seconds to stabilize the cart displacement. The author has also tried the same with the angular displacement of the link as Figure 5.17 shows and it took in the cyclic disturbance of 10 seconds for a total of 100 seconds, 9.3 seconds to stabilize.

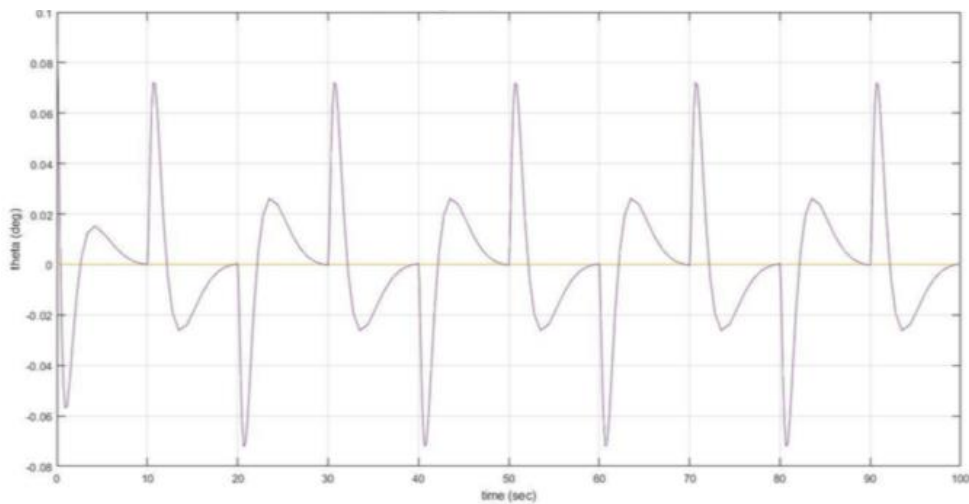


Figure 5.17: cyclic disturbance for angular displacement of the link q_2

It is important to tune the Q and R in order to get the optimal control one desires for such control of the inverted pendulum. As a conclusion of vibration control results, the LQR controller stabilized the cart of the inverted pendulum which means that the LQR is effective to control the inverted pendulum vibration and get it back to the stabilized state.

5.5 Maximum Pelvis Mass Stability

The author has conducted an extra experiment in order to see how the robot can walk with maximum pelvis density possible. The result that was received is that the robot can walk and stand with a stability whether dynamic or static up to 500 kg/m^3 . However, the robot couldn't control its balance when the density exceeded 1000 kg/m^3 .

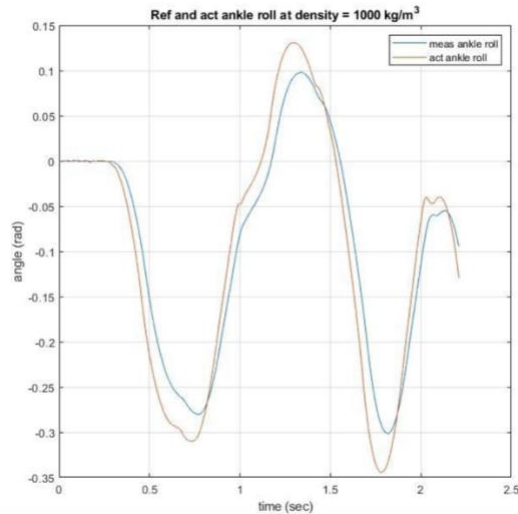


Figure 5.18: ankle roll joint vs time

Figure 5.18 shows that the robot made only 2 steps and then it fell on the floor after 2.212 seconds because it couldn't control itself with high pelvis density of 1000 kg/m^3 .

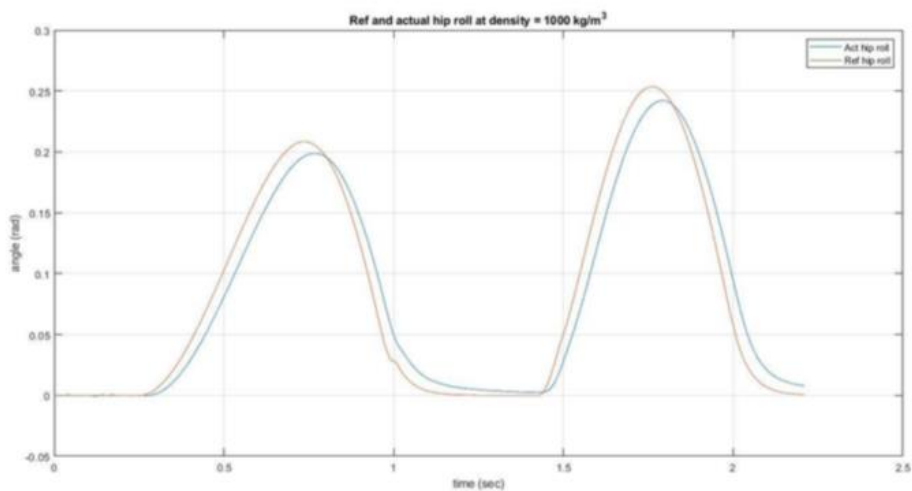


Figure 5.19: hip roll joint vs time

This Figure 5.19 shows also that after 2.212 seconds the hip roll joint stopped after the robot fell down on floor because of the high density.

5.6 Future Work

The bipedal robot movement balance is really a challenging topic. In order to tackle this problem, several scientists around the world are trying to develop different models as the bipedal robot would exist in our future helping the mankind in different hard tasks. Several literature papers have suggested different concepts in order to balance the bipedal robot dynamically and statically. However, based on the simulations and results, it is recommended to have further investigations and future work should be conducted in order to have better performance.

- Regarding the vibration control, it is needed to develop another model which is trending now in the latest papers which is the inverted pendulum plus flywheel since that it is close to the reality of the complexity of the bipedal robot movement. This model requires an even stronger controller development like the fuzzy linear quadratic regulator since that it has better performance in settling time, peak overshoot, steady state error and RMSE.
- According to the results of the extra mass of pelvis, it is preferred to develop a controller along with the MPC used so that it works with all masses and all designs.
- According to the PID's results for the dynamic time response for the joints, the model should be improved to avoid errors in angles neither time delay.
- The author has assumed that the walking gait is a straight line; however, it is realistic to explore more and try to make the robot walk in different paths. It should be simulated in different directions of walking.
- The author has assumed that the external perturbations are applied on the pelvis, however, in real life sudden external perturbations can be even applied to the legs; thus, further investigations should be conducted to explore more and try to control all the sudden vibrations applied on any part of the robot.
- The plane was assumed to be frictionless; however, the robot should be also tested on rough terrain because mostly the environment we live in has friction, thus the dynamic and static balance would differ at that point.

- Simulation is the ideal environment; however, implementing a physical raptor dinosaur robot that can perform all the balancing and controlling that were designed is more realistic to see how the simulation can become reality.
- Further investigations may be applied to develop machine learning so that the physical prototype of the robot may decide how to walk and how to avoid obstacles and how to behave like a real animal.

SUMMARY

The thesis paper has been conducted for educational purpose. The balance of the bipedal robots' movement is really a challenging topic. In order to tackle this issue, such models and strategies should be put to prevent falling on ground. The balance of bi-legged walking robots should be done on the dynamic and static aspects to keep the walking gait trajectory stable. It is also important to put into consideration the external perturbations in the surrounding environment of the robot gait since they may cause loss of balance. Lateral vibrations applied to the skeleton should be controlled in order to make the robot stable.

In this thesis paper, the author has tackled these problems in different scientific methodologies. Extensive research has been conducted on most updated literature review papers that tackle this subject. Suitable model has been selected on which the designed robot stabilizes against the external perturbations. From the mathematical perspective, the equation of motion and linearizing the nonlinear system have been derived. Designing the suitable controller was in that case the linear quadratic regulator due to its robustness and effectiveness in maintaining such stability for the pelvis against vibrations.

Following through, the 3D robot skeleton has been designed along with balancing controllers block diagrams to maintain the dynamic and static stability. The MPC kept the dynamic and static balance of the bipedal robot in both the DSP and the SSP while stepping in the simulation through anticipating the future motion in the future horizon.

The results received during the simulation and analysis were successful. The LQR controller could handle the vibration; while, the MPC could maintain the dynamic and static balance; which are the core of this thesis. A lot of recommendations have been set up after experimenting different scenarios. Further investigations should be studied in order to improve the bipedal robot walking gait closer to the human-like scenarios and activities. The journey of balancing bipedal robots' movement is long; and periodically, enhanced systems and algorithms are being developed by scientists to make the bipedal robots act and behave like us.

KOKKUVÕTE

See lõputöö on koostatud hariduslikul eesmärgil. Kahejalgsete robotite liikumise tasakaal on tõesti komplitseeritud teema. Selle probleemi lahendamiseks tuleks välja töötada sellised mudelid ja strateegiad mis väldiksid roboti ümber kukkumist. Kahe jalaga kõndivate robotite tasakaal peaks olema dünaamiline ja staatiline, et trajektoor püsiks stabiilne. Väga oluline on arvestada ümbritsevat keskkonda ja väliseid tegureid, mis võivad mõjutada robotite kõnnakut ja kaotada nende tasakaalu. Luustikule rakenduvaid külgmisi vibratsioone tuleks kontrollida, et robot oleks stabiilne.

Selles lõputöös on autor käsitlenud neid probleeme läbi erinevate teadusmetoodikate. On läbi viidud ulatuslikud uuringud selle teemaga tegelevate kõige uuemate akadeemiliste artiklite kohta. Valitud on sobiv mudel, millel disainitud robot stabiliseerub väliste mõjutuste vastu. Matemaatilisest vaatenurgast on tuletatud liikumise võrrand ja mittelineaarse süsteemi lineariseerimine. Sobiva kontrolleri kavandamine oli sel juhul lineaarne ruutregulaator tänu oma robustsusele ja efektiivsusele vaagnaluule, säilitades stabiilsust vibratsioonide eest.

Dünaamilise ja staatilise stabiilsuse säilitamiseks on 3D-roboti skelett kavandatud koos tasakaalustus regulaatorite plokk skeemidega. MPC hoidis kõndimissimulatsioonil kahejalgse roboti dünaamilist ja staatilist tasakaalu nii DSP-s kui ka SSP-s, nähes ette liikumist tulevikus.

Simulatsioonide ja analüüside käigus saadud tulemused olid edukad. LQR kontrolleri valitses vibratsioone õnnestunult; samas säilitas MPC dünaamilise ja staatilise tasakaalu; mis on selle lõputöö tuumik. Pärast erinevate stsenaariumide katsetamist on koostatud palju soovitusi. Täiendavad uuringud tuleks läbi viia, et parandada kahejalgsete robotite kõnnakut mis sarnaneb rohkem inimlaadsetele stsenaariumidele ja tegevustele. Kahepoolsete robotite liikumise tasakaalustamise teekond on pikk; perioodiliselt teadlased töötavad välja täiustatud süsteeme ja algoritme, et panna kahejalgsed robotid tegutsema ja käituma nagu meie.

LIST OF REFERENCES

1. White, J., Swart, D., & Hubicki, C. (2020). Force-based Control of Bipedal Balancing on Dynamic Terrain with the Tallahassee Cassie Robotic Platform. *Proceedings - IEEE International Conference on Robotics and Automation*, 6618–6624.
2. Snafii, N., Abdolmaleki, A., Lau, N., & Reis, L. P. (2015). Development of an Omnidirectional Walk Engine for Soccer Humanoid Robots. *International Journal of Advanced Robotic Systems*, 12(12).
3. Ott, C., Roa, M. A., & Hirzinger, G. (2011). Posture and balance control for biped robots based on contact force optimization. *IEEE-RAS International Conference on Humanoid Robots*, 26–33.
4. Bahdi, E. (2018). Development of a Locomotion and Balancing Strategy for Humanoid Robots. 90.
5. VUKOBRATOVIĆ, M., & BOROVIĆ, B. (2004). Zero-Moment Point — Thirty Five Years of Its Life. *International Journal of Humanoid Robotics*, 01(01), 157–173.
6. Vaz, J. C., & Oh, P. (2020). Material Handling by Humanoid Robot while Pushing Carts Using a Walking Pattern Based on Capture Point. *Proceedings - IEEE International Conference on Robotics and Automation*, 9796–9801.
7. Warnecke, D., Meßmer, M., de Roy, L., Stein, S., Gentilini, C., Walker, R., Skaer, N., Ignatius, A., & Dürselen, L. (2019). Articular cartilage and meniscus reveal higher friction in swing phase than in stance phase under dynamic gait conditions. *Scientific Reports*, 9(1), 1–9.
8. Al-Shuka, H. F. N., Corves, B. J., Vanderborght, B., & Zhu, W.-H. (2014). Zero-Moment Point-Based Biped Robot with Different Walking Patterns. *International Journal of Intelligent Systems and Applications*, 7(1), 31–41.
9. Yu, Z., Chen, X., Huang, Q., Zhang, W., Meng, L., Zhang, W., & Gao, J. (2016). Gait Planning of Omnidirectional Walk on Inclined Ground for Biped Robots. *IEEE Transactions on Systems, Man, and Cybernetics: Systems*, 46(7), 888–897.

10. Wang, P., Liu, G., Zha, F., Guo, W., Li, M., & Cai, H. (2016). A simple control algorithm for controlling biped dynamic walking with stopping ability based on the footed inverted pendulum model. *Advances in Mechanical Engineering*, 8(9), 1–12.
11. Denisov, A., Iakovlev, R., Mamaev, I., & Pavliuk, N. (2017). Analysis of balance control methods based on inverted pendulum for legged robots. *MATEC Web of Conferences*, 113, 1–6.
12. Ding, B., Plummer, A., & Irvani, P. (2016). Investigating Balancing Control of a Standing Bipedal Robot With Point Foot Contact. *IFAC-PapersOnLine*, 49(21), 403–408.
13. Elhaisri, A. I., Centre, S. S., & Sciences, P. (2015). Humanoid Robot Full-Body Control & Balance Restoration. June.
14. Dehart, B. J., & Gorbet, R. (2019). Dynamic Balance and Gait Metrics for Robotic Biped by. Thesis, June.
15. Zhang, L., & Fu, C. (2018). Predicting foot placement for balance through a simple model with swing leg dynamics. *Journal of Biomechanics*, 77, 155–162.
16. Joe, H. M., & Oh, J. H. (2018). Balance recovery through model predictive control based on capture point dynamics for biped walking robot. *Robotics and Autonomous Systems*, 105, 1–10.
17. Reimann, H., Fettrow, T., & Jeka, J. J. (2018). Strategies for the control of balance during locomotion. *Kinesiology Review*, 7(1), 18–25.
18. Shafiee-Ashtiani, M., Yousefi-Koma, A., Shariat-Panahi, M., & Khadiv, M. (2017). Push recovery of a humanoid robot based on model predictive control and capture point. *4th RSI International Conference on Robotics and Mechatronics, ICRoM 2016*, 433–438.
19. Araffa, K., & Tkach, M. (2019). Implementation and simulation a model predictive control for motion generation of biped robot. *Adaptive Systems of Automatic Control*, 2(35), 3–12.
20. Roose, A. I., Yahya, S., & Al-Rizzo, H. (2017). Fuzzy-logic control of an inverted pendulum on a cart. *Computers and Electrical Engineering*, 61, 31–47.

21. Abut, T., & Soyguder, S. (2019). Real-time control and application with self-tuning PID-type fuzzy adaptive controller of an inverted pendulum. *Industrial Robot*, 46(1), 159–170.
22. Marada, T., Matoušek, R., & Zuth, D. (2017). Design of linear quadratic regulator (LQR) based on genetic algorithm for inverted pendulum. *Mendel*, 23(1), 149–156.
23. Fauziyah, M., Amalia, Z., Siradjuddin, I., Dewatama, D., Wicaksono, R. P., & Yudaningtyas, E. (2020). Linear quadratic regulator and pole placement for stabilizing a cart inverted pendulum system. *Bulletin of Electrical Engineering and Informatics*, 9(3), 914–923.
24. Hazem, Z. Ben, Fotuhi, M. J., & Bingül, Z. (2020). Development of a Fuzzy-LQR and Fuzzy-LQG stability control for a double link rotary inverted pendulum. *Journal of the Franklin Institute*, 357(15), 10529–10556.
25. Jing, C., & Zheng, J. (2020). Stable walking of biped robot based on center of mass trajectory control. *Open Physics*, 18(1), 328–337.
26. Ding, J., Xin, S., Lam, T. L., & Vijayakumar, S. (2021). Versatile Locomotion by Integrating Ankle, Hip, Stepping, and Height Variation Strategies. *Icra*.
27. Aftab, Z., Robert, T., & Wieber, P. B. (2012). Ankle, hip and stepping strategies for humanoid balance recovery with a single Model Predictive Control scheme. *IEEE-RAS International Conference on Humanoid Robots*, 159–164.